

~~SECRET~~
~~SECRET~~
ERDA/JPL-954412-77/
Distribution Category UC-63

SILICON MATERIAL TASK, PART III LOW-COST SILICON SOLAR ARRAY PROJECT

Texas Instruments Report No. 03-77-05

Final Report

R. A. Roques
D. M. Coldwell

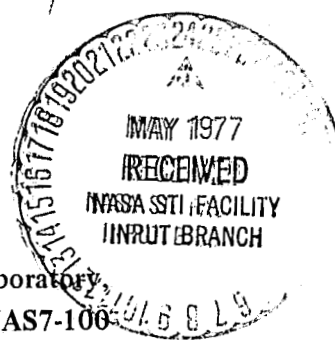
January 1977



JPL Contract No. 954412



Texas Instruments Incorporated
P.O. Box 5012
Dallas, Texas 75222



This work was performed for the Jet Propulsion Laboratory, California Institute of Technology, under NASA Contract NAS7-100 for the U.S. Energy Research and Development Administration, Division of Solar Energy.

The JPL Low-Cost Silicon Solar Array Project is funded by ERDA and forms part of the ERDA Photovoltaic Conversion Program to initiate a major effort toward the development of low cost solar arrays.

Page intentionally left blank

ABSTRACT

The feasibility of a process for carbon reduction of low impurity silica in a plasma heat source was investigated to produce low-cost (<\$10 per kilogram) solar-grade silicon. Theoretical aspects of the reaction chemistry were studied with the aid of a computer program using iterative free energy minimization. These calculations indicate a threshold temperature exists at 2400 K below which no silicon is formed. The computer simulation technique of molecular dynamics was used to study the quenching of product species.

Initial experiments using vendor's plasma equipment verified that silica could be reduced to silicon with carbon, provided sufficient residence time was permitted. Feeding the SiO_2/C mixture to the plasma reactor in rod form allowed sufficient time for small amounts of silicon product to be identified.

An experimental laboratory-scale plasma reactor was fabricated and used to optimize process variables for reaction conditions which yielded the maximum amount of silicon product. The conditions for maximum yield were 14 kW power, 3 liters/min plasma gas flow, and reactant feed rate of 0.02 gm/min. Maximum silicon content, measured by wet analysis, of the sintered condensate was 33%. Reactant mixtures which yielded the greatest amount of silicon were those containing between 1.5:1 and 1.9:1 carbon to silica mole ratios. Silicon was observed to form "in-situ" on the tip of the feed rod of mixtures containing optimum reactant quantities.

Emission spectrographic analysis of the silicon product showed a reduction in impurity level of one to two orders of magnitude from that present in the starting materials. Electrically active elements such as boron, arsenic, and phosphorus were below the detectable limits of emission spectroscopy.

Page intentionally left blank

Intensity measurements using spectrographic techniques were made for mapping the temperatures at various levels in the plasma flame. A steep temperature gradient from 15,000 K to 600 K was observed.

The plasma approach proved technically feasible to produce relatively pure silicon. However, the results from this very small scale unit suggest a highly inefficient energy utilization due to poor heat transfer characteristics of the plasma flame coupled with a low overall yield of recoverable silicon indicate the process to be economically unattractive. Carbon monoxide and CO_2 in the exhaust gases and silicon content of the product condensate support the identified condensed-phase reaction mechanism.

TABLE OF CONTENTS

<i>Section</i>	<i>Title</i>	<i>Page</i>
I.	INTRODUCTION	1
II.	ANALYSIS OF REACTION CHEMISTRY	5
	A. Thermodynamic Considerations	5
	1. Computational Techniques	5
	2. Results and Discussion	7
	a. Computed Optimization of Carbon Content	8
	b. Heat Transfer Considerations	11
	3. Summary of Thermodynamic Analysis	11
	B. Molecular Dynamics of Product Quenching	11
	1. Computational Technique	12
	2. Simulation Results	12
	3. Summary	16
III.	TECHNICAL DISCUSSION	17
	A. Raw Material Selection	17
	B. Laboratory Preparation of Raw Materials	17
	C. Raw Material and Prepared Batch Analysis	19
	D. Preparation of Raw Material Mixtures	21
	1. Pelletized Batch for Pilot Scale Run	21
	2. Material Preparation for Solid Feed Rod	21
	E. Plasma Tests Using Vendor's Equipment	22
	1. Material Preparation for IONARC Furnace Test	23
	2. IONARC Furnace Tests	23
	3. DC Torch Tests	26
	4. Results of Additional Tests	28
	F. Design and Fabrication of Experimental Reactor	30
	1. Experimental Reactor Description	30
	2. Reactor Design Modifications	31
	3. Flame Temperature Mapping	34

TABLE OF CONTENTS (Continued)

<i>Section</i>	<i>Title</i>	<i>Page</i>
G.	Experimental Plasma Reactor Tests	37
1.	Scoping Experiments	37
a.	Methane Experiment (Gaseous Form of Carbon)	38
b.	Reduced Carbon Content in Mixture	40
c.	Cold Versus Hot Quenching Temperature	40
d.	Analysis of Reaction By-Product Gases	40
2.	Plan for Experimental Reactor Study	41
3.	Matrix of Experiments for Optimization of Variables	41
a.	Design of Statistical Experiments	41
b.	Experimental Results	43
c.	Variation of Feed Material Composition	45
d.	Product Consolidation and Analysis	47
e.	In-Situ Formation of Silicon on Feed Rod	48
4.	Discussion of Results	49
a.	Observations on Quenched Product Characteristics	49
b.	Factors Contributing to Silicon Yield	50
c.	Observed Reaction in the Plasma and Interpretation of Reaction Mechanism	51
IV.	PRELIMINARY ECONOMIC STUDY	53
V.	CRITICAL ASSESSMENT	55
A.	Contributions	55
B.	Identified Obstacles	55
VI.	CONCLUSIONS AND RECOMMENDATIONS	57
VII.	PROGRAM SCHEDULE	59
VIII.	REFERENCES	61

APPENDICES

- A. EVALUATION CRITERIA
- B. EMISSION SPECTROGRAPHIC DETECTION LIMITS FOR IMPURITIES
IN SILICON AND CARBON
- C. DETECTION LIMITS FOR IMPURITIES IN SILICON
- D. PROCEDURE FOR DETERMINATION OF SILICON

LIST OF ILLUSTRATIONS

<i>Figure</i>	<i>Title</i>	<i>Page</i>
1.	Solar Silicon Production with Plasma	3
2.	Free Energies of Possible Reactions in Si-O-C System	6
3.	Yield Versus Reaction Temperature	7
4.	Isotherms – 2500-6000 K	8
5.	Production of SiO and SiC (at 2.0 moles carbon)	10
6.	Reaction Products Below the Threshold Temperature	10
7.	Free Energy Change Upon Quenching	14
8.	Formation of Silicon Upon Quenching	14
9.	Amount of Sintered Silicon Upon Quenching	15
10.	Silica/Carbon (2.5:1 wt ratio) Raw Material Mixture Photomicrograph	18
11.	Carbon Particles Coating Silica (500X) – SEM	19
12.	Pelletized SiO ₂ -C Mixture	22
13.	350-Kilowatt IONARC DC Plasma Furnace	24
14.	DC Plasma Experimental Setup for Solid Feed Rod	29
15.	Experimental RF Plasma Reactor	30
16.	Effect of Sheath Gas Flow on Plasma Flame	31
17.	Improved Design of Induction Plasma Reactor	32
18.	Experimental Induction Plasma Reactor	33
19.	Equipment Diagram for Temperature Measurement	34
20.	Temperature Profile of Plasma Flame	38
21.	Planned Approach for Reactor Studies	42
22.	Schematic Representation of Experiments	43
23.	Silicon Globules Produced by Consolidation of Material Collected from Plasma Reaction	47
24.	Tip of Feed Rod Converted to Silicon – Run P-50, Batch B-17	48
25.	Vertical Induction Furnace for Silicon Smelting Process	58
26.	Program Schedule	59

LIST OF TABLES

<i>Table</i>	<i>Title</i>	<i>Page</i>
1.	Manufacturing Cost Estimate	1
2.	Energy Cost Estimate	2
3.	Isotherm Slopes	9
4.	Emission Spectrographic Analysis of Raw Materials	17
5.	Emission Spectrographic Analysis of Raw Materials	20
6.	Emission Spectrographic Analysis of Mixtures (ppm wt) Prepared in Laboratory and J. M. Huber Corporation	20
7.	IONARC Furnace Tests	25
8.	Experiments Using DC and RF Torch	27
9.	Analytical Results of Reaction Product from Plasma Tests	28
10.	Analytical Results of Reaction Products	29
11.	Scoping Experiments with Induction Plasma Reactor	39
12.	Results of Experiments for Optimization of Variables	44
13.	Variation in Composition and Batch Preparation of Feed Mixture	46
14.	Emission Spectrographic Analysis of Silicon	48

SECTION I INTRODUCTION

The objective of the Silicon Material Task, Part III, of the Low-Cost Silicon Solar Array Project is to produce solar-grade polycrystalline silicon at a cost of less than \$10 per kilogram. This is prerequisite to the 1985 goal established by ERDA for a solar array selling price of \$500 per kilowatt.

The approach taken toward this objective was the reduction of low-impurity silica with carbon in the plasma heat source. The direct reduction of silica with carbon is the reaction on which metallurgical-grade silicon is based and is currently being produced.¹ The reduction of silica with carbon is thermodynamically favored over other nonmetals, e.g., H₂, S and P and of the group 1A alkali metals (Li, Na and K), only Li is a feasible reducing agent.² The raw materials were high purity commercially available silica and carbon. Contamination was minimized during the reduction process. A plasma reactor using an inert gas such as argon, offered a noncontaminating source of high-temperature heat for carrying out the reduction reaction. Forethought was given to the high-volume, low-cost aspects of the production process when considering raw material preparation and handling. The final silicon product was needed in a form amenable to the crystal growth process as currently practiced in the semiconductor industry.

Economics and energy conservation were important considerations and some preliminary estimates were made for this approach. Tables 1 and 2 are initial estimates made of the manufacturing costs and energy utilization.

Table 1. Manufacturing Cost Estimate

Raw Material Costs		
Silica	\$0.077/kg	
Carbon	0.35/kg	
Raw Material Costs per kg of Silicon		\$0.48
Raw Material Preparation Costs		0.55
Plasma Processing Costs		<u>2.20</u>
Total Estimated Cost per kg of Silicon		\$3.23

Table 2. Energy Cost Estimate
(Based on producing 1 Kg of silicon slices, 0.2 mm thickness)

Process	SC-Grade Si Current Process	Solar-Grade Si Plasma Process
Sawing, Polishing	32 kWh	32 kWh
Crystal Growth	416	416
Deposition	2140	0
Reaction, Purification	20	0
Smelting	500	40
Transportation, Mining	0.2	0.2
	<hr style="width: 50%; margin: 0 auto;"/> 3108.2 kWh	<hr style="width: 50%; margin: 0 auto;"/> 488.2 kWh

In order to maximize reactivity of the raw materials, fine grinding and intimate blending are first necessary. The silica was purchased as silica flour of less than 400 mesh ($<37 \mu\text{m}$) particle size and the carbon, i.e., carbon black, is available in a pelletized form of ultimate particle size in the millimicron range. The raw materials can be further comminuted and blended in a ball mill using flint pebble grinding media and rubber-lined mills to minimize contamination of the silica and carbon. The general approach taken therefore was the upgrading of starting material quality and process equipment, adaption to production methods for handling large volumes of material at low cost, and careful avoidance of contamination of the reactants and product throughout the process. The silicon produced was significantly purer than currently available metallurgical-grade material and projected to be of sufficiently low impurity level to qualify as solar-grade polysilicon. A simplified process, which does not indicate several intermediate steps required, is shown diagrammatically in Figure 1.

Several articles on plasma technology as related to this process are in the literature.

Reed³ describes an induction-coupled plasma torch which is vortex stabilized. This is accomplished by feeding the gas tangentially into the tube causing it to spiral down the walls and generally contributing to recirculation of the plasma and cooling of the tube wall. A spectrographic technique was used for measuring the plasma temperature. An energy distribution was developed which indicates 52-57% of the total power is transferred to the plasma from the high-voltage source.

Boumans, deBoer, and deRuiter⁴ used a stabilized RF argon plasma for emission spectroscopy. They designed a plasma torch and generator system which operated at a power level of 1 to 2 kW and at a frequency of about 50 MHz. The flame parameters were controlled to produce a toroidal structure which facilitated feeding fine particles into the hot zone.

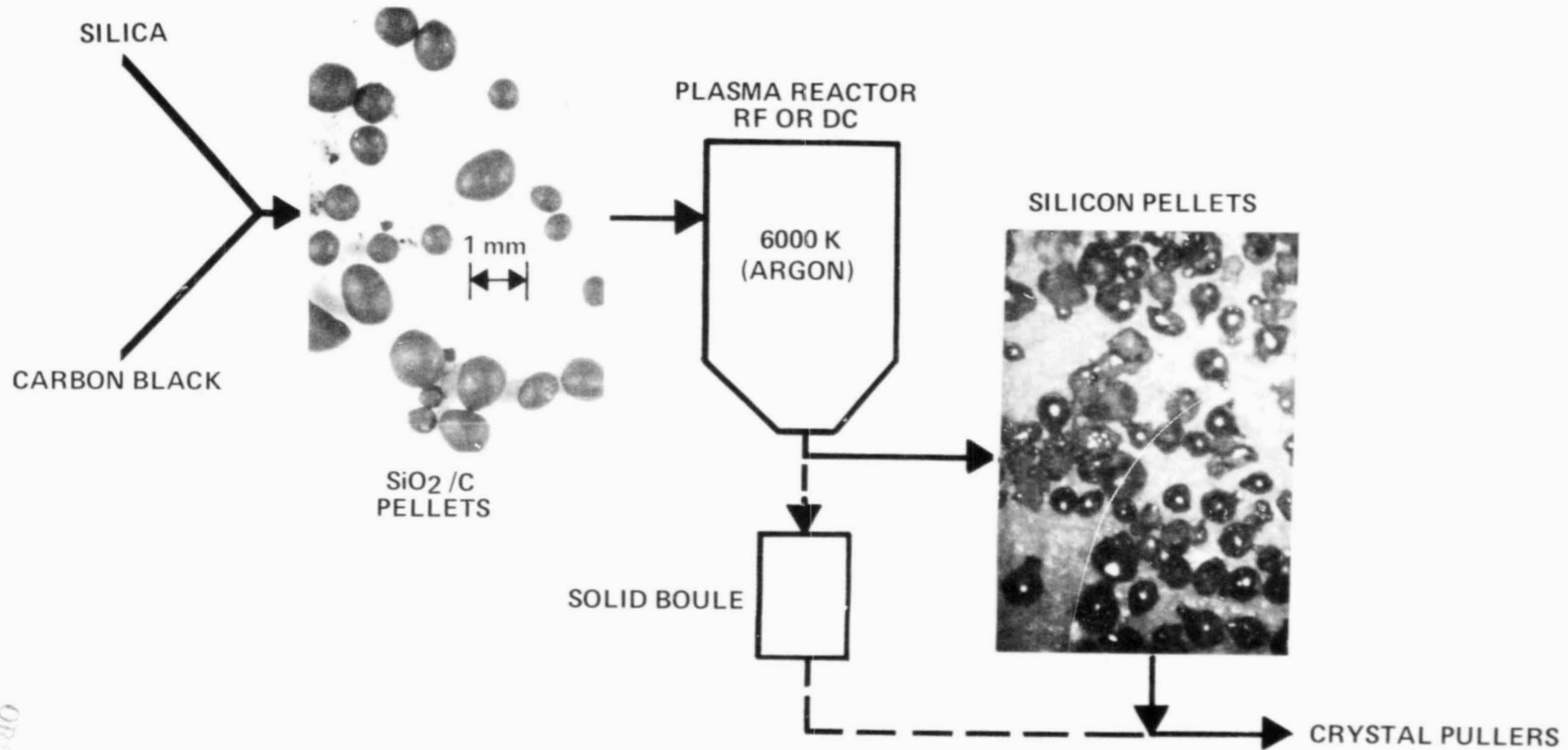


Figure 1. Solar Silicon Production with Plasma

ORIGINAL FROM
OF 1975

An induction plasma reactor was used experimentally by Rains and Kadlec⁵ for reduction of aluminum oxide to aluminum. Effects of particle size of the Al_2O_3 , powder flow rate, and power input on percent conversion of the alumina were measured. The effects of introducing H_2 , CO , and CH_4 into the argon plasma were also studied. Al containing species were identified in the plasma flame by use of a spectrograph.

Nassau and Shiever⁶ made a laboratory study of the process used for producing high-purity silica by the oxidation of SiCl_4 in an induction plasma.

Other studies⁷ have been made with the applications of plasma technology to chemical processing in which the noncontaminating aspects of the RF plasma torch, theoretical considerations in the reactor design, and procedural methods have been reported.

Three general objectives of the technical effort in this program were:

- 1) Demonstrate the feasibility of the reduction of silica to silicon with carbon as the reductant using an inert gas plasma source;
- 2) Make a manufacturing cost estimate based upon a 3000 MT per year production of silicon;
- 3) Provide recommendations for dealing with environmental problems which may be associated with the process.

Specific objectives and criteria for directing progress on the program are included in the Evaluation Criteria which may be found in Appendix A of this report.

SECTION II ANALYSIS OF REACTION CHEMISTRY

A. THERMODYNAMIC CONSIDERATIONS

The desired reaction combines silica (SiO_2) and carbon forming elemental silicon and carbon monoxide. This reaction is complicated by the possible formation of other undesired products. The metallurgical industry has studied these reactions and their associated levels of contamination in connection with the arc-furnace approach.⁸ Other than the basic considerations of this work, no theoretical references have been found.

Calculations were made considering condensed-condensed, condensed-vapor and vapor-vapor reactions with no distinction made between solid and liquid. While this model does not exactly predict results from a specific experimental condition since the reaction kinetics are not known, it does give an indication of the possibility of reaction, and an estimation of the maximum yield of the system. The model assumes equilibrium is achieved, which is unlikely in an actual reaction. The indicated results should be valid in the case of a plasma which has an extremely high temperature (>6000 K) and very small particles ($<200 \mu\text{m}$) of a stoichiometric mixture of silica and carbon. With sufficient residence time in the plasma, the particles should reach the average plasma temperature throughout and approach the equilibrium product state.

While this model is aimed at the problem of producing solar-grade silicon, it is also applicable to the metallurgical silicon process or any other silica reduction reaction utilizing carbon. The calculations include the basic reduction reaction and possible side reactions, an advantage of this model over simple one reaction free energy calculations. From the large number of possible reactions the most feasible ones that minimize the free energy at a particular temperature are "allowed" to occur.

1. Computational Techniques

Modified versions of a computer program described by Cruise⁹ and used by Hunt and Sirtl¹⁰ were used to investigate the equilibrium concentration of reactants in the chemical reaction. The free energy of the system was minimized by varying the concentration of each of the components of the system (elemental or molecular) while holding the remainder fixed. The calculation was iterative through the list of components until the equilibrium constants (calculated from the free energies) differed from the apparent equilibrium constants (calculated from the molar amounts of

the species present) by a predetermined constant. Any species whose molar concentration fell below another set constant was automatically excluded from the calculation.

The input to the program requires that the initial amounts of each species be specified and are kept constant throughout that calculation. It was simpler to fix the initial estimate of the composition and then vary the temperature rather than vice-versa since the initial estimate was independent of the final distribution of the elements among the possible molecular configurations. The results included the molar composition, the equilibrium constant calculated, and the partial pressures of each species in tabular form.

The thermodynamic data used in these calculations were obtained from the *JANAF Thermochemical Tables*.¹¹ These data are valid in the range 500 to 6000 K. A regression analysis was performed on the heat capacities, entropies, and enthalpies of the elements and compounds considered so that the data would be easily retrievable at any temperature selected.

Using the JANAF data directly, possible reactions were plotted in Figure 2 to demonstrate the complexity of this system and to observe the approximate temperatures at which the reactions considered would be expected to proceed. The desired reaction of the direct stoichiometric

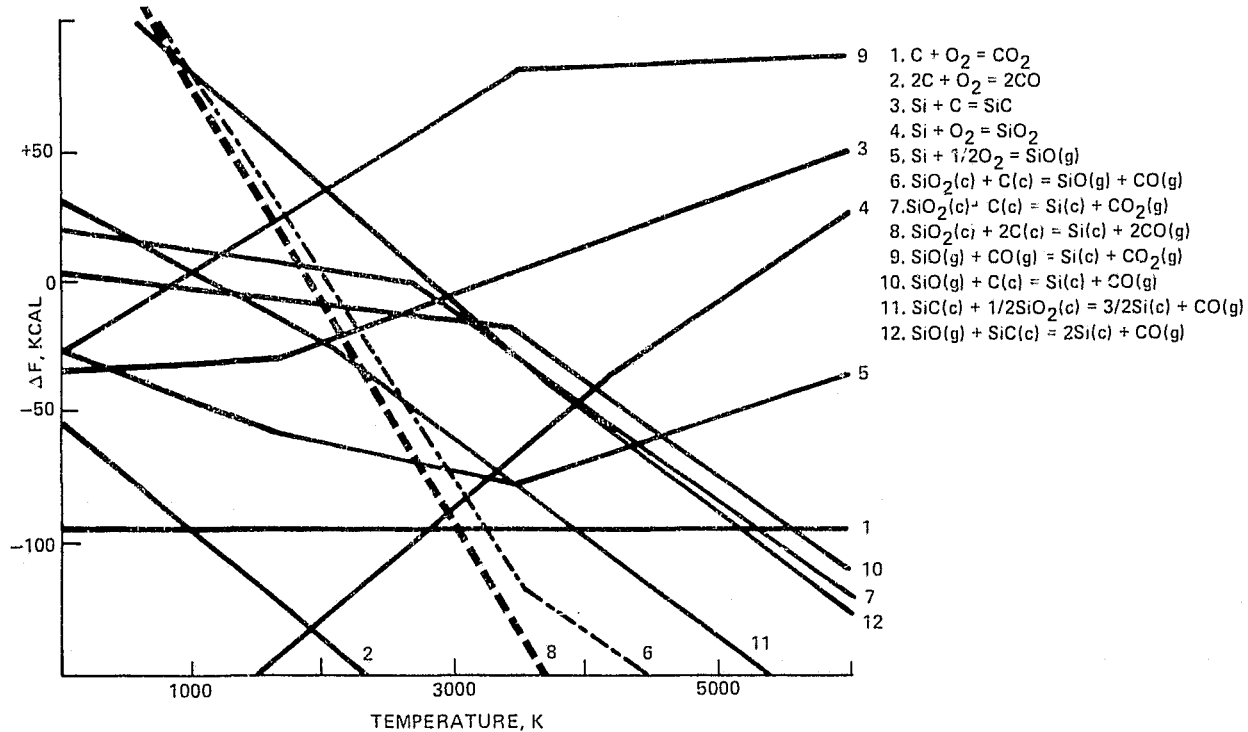


Figure 2. Free Energies of Possible Reactions in Si-O-C System

reduction of silica with carbon, reaction eight of Figure 2, becomes favorable at approximately 1900 K. Below this temperature, the major products were calculated to be silicon carbide, silicon monoxide, and unreacted silica. The silicon carbide reaction becomes unfavorable around 3250 K while the silicon monoxide reaction remains favorable until much higher temperatures. The reduction of silica to elemental silicon is only slightly more favored than the production of silicon monoxide.

2. Results and Discussion

Computations were performed over a range of temperatures from 500 to 6000 K at a constant pressure of one atmosphere. In the initial model of the system, carbon and silica were considered solids exposed to the specified temperature which determined whether the reactants or products would vaporize or remain in their condensed state. The compounds of the three base elements, Si, C, O, considered were SiO, SiO₂, SiC, CO, CO₂, and O₂. These nine species were the only ones allowed to exist at any temperature. The thermodynamics determined how much, if any, of each was present.

The computer-generated data show a sharp rise in the yield of silicon even when reactants were mixed in nonstoichiometric ratios, i.e., silica to carbon ratios of greater than one half. Figure 3

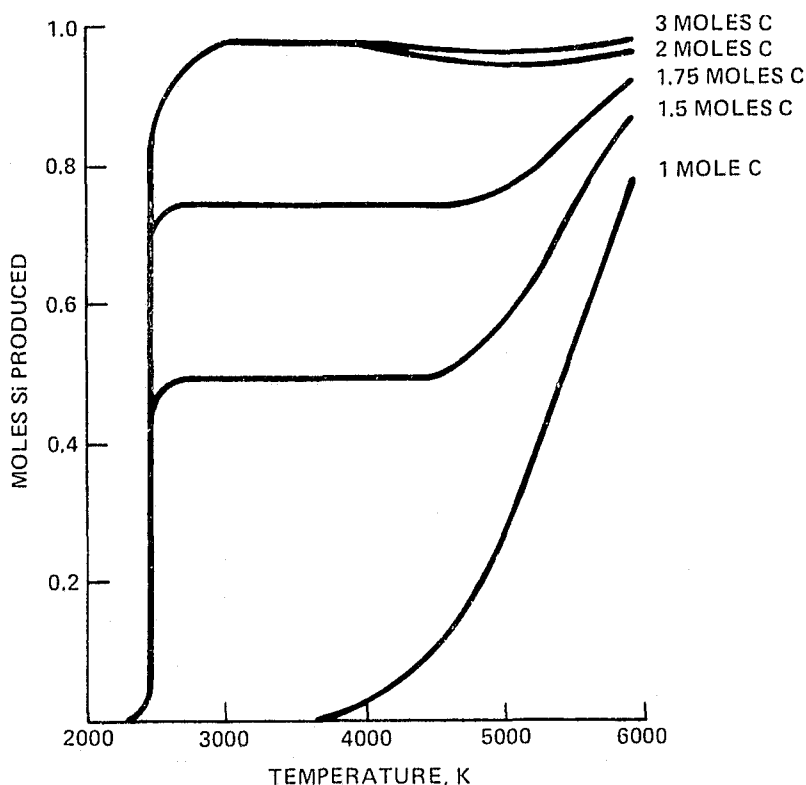


Figure 3. Yield Versus Reaction Temperature

illustrates the results of these calculations and shows that a threshold temperature occurs between 2400 and 2500 K. The silica reduction reaction proceeds to silicon only when the temperature is above this threshold. The marked rise in yield of silicon is visible only for carbon contents greater than one mole carbon since a higher temperature reduction yielding silicon and carbon dioxide (reaction seven of Figure 2) is favored at this ratio. When the carbon content is increased above this level, the threshold and a nearly uniform plateau are observed. The yield between 2500 and 4500 K is relatively constant until all the reactants become gaseous, at which time, the yield increases.

In all these calculations, the change of phase from condensed to gaseous is considered along with the resulting changes in partial pressures and associated free energies. When a calculation was made using ideal gas values for the free energy, the threshold temperature shifted upward. This difference indicates that, while a gaseous reaction can occur, a reaction to form silicon is possible even when carbon does not have a significant vapor pressure. The reaction was observed to occur while elemental silicon and carbon are both in their condensed forms.

a. Computed Optimization of Carbon Content

Isotherms of the moles of silicon produced with varying amounts of carbon were also obtained and represented in Figure 4. When reactants are in their condensed phases, the production of silicon

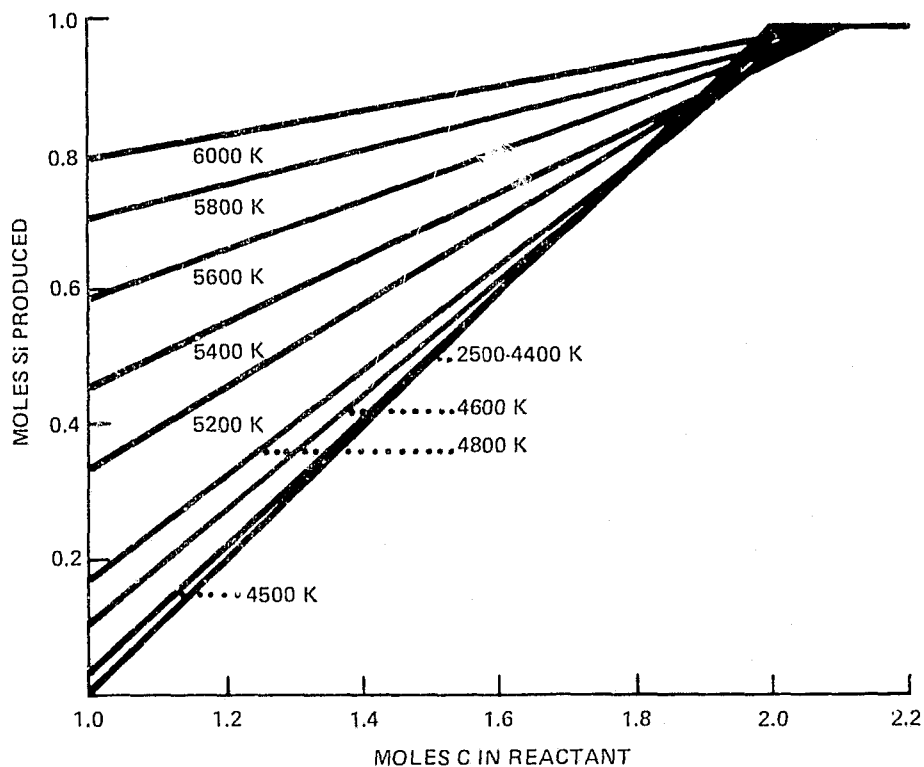


Figure 4. Isotherms - 2500-6000 K

follows the 2500-4400 K isotherm. Carbon becomes vapor above 4473 K and a vapor phase reaction takes place and increases in rate with temperature. The slopes of curves are given in Table 3. From an analysis of this table, it can be seen that the rate of silicon formation with carbon increases as:

$$\frac{dS}{dT} = -4.97 \times 10^{-4} T + 3.148$$

where S is the slope of the isotherms of Figure 4 and T is temperature.

Table 3. Isotherm Slopes

Temperature (K)	Slope
2500-4400	0.981
4500	0.882
4600	0.842
4800	0.774
5200	0.585
5400	0.470
5600	0.354
5800	0.249
6000	0.167

The optimum amount of carbon to be added to the silica is approximately two moles. This provides enough carbon to promote the lower temperature reduction giving off carbon monoxide. While the yield is higher by three to four percent with three moles carbon added, unreacted carbon contaminates the product with the possibility of a reaction resulting in silicon carbide as the product cools. The isotherms of Figure 4 converge at a maximum yield at 2.05 moles carbon. With this amount, the silicon yield is maximized for any temperature above the threshold. The contamination of the product with silicon monoxide and silicon carbide is minimized at two moles of carbon at temperatures between 2500 and 3000 K. This is also the region of nearly maximum yield and gives liquid silicon product, which might simplify product collection procedures. The production of silicon monoxide and silicon carbide with temperature are depicted in Figure 5.

Below the threshold temperature, Figure 6 shows the production curves of silicon carbide, silicon monoxide, and unreacted silicon dioxide at 2000 K. The silicon dioxide is consumed by the reaction forming silicon carbide and silicon monoxide until 2.38 moles carbon when all silicon dioxide has been reacted. The silicon carbide then increases with increasing carbon content at the expense of silicon monoxide.

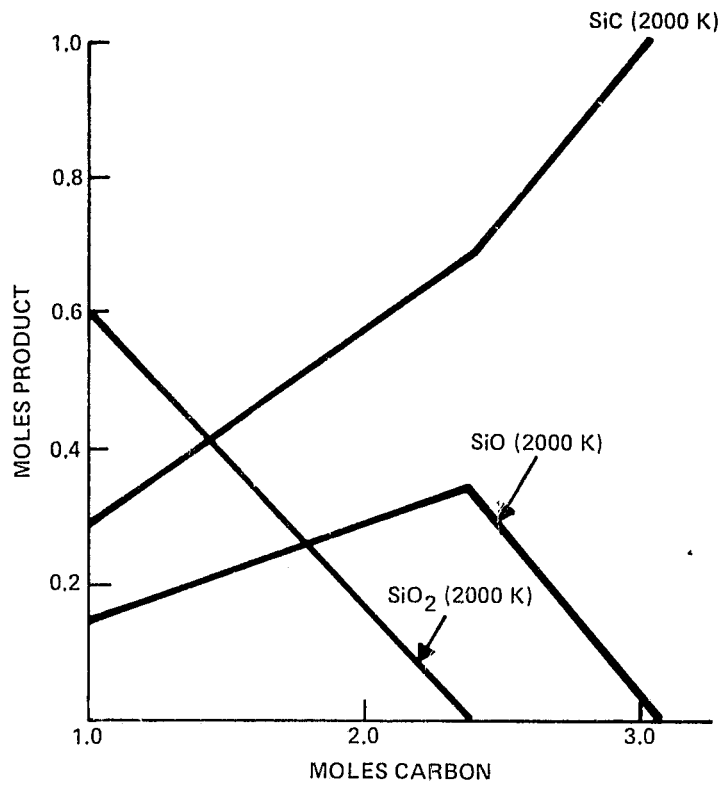


Figure 5. Production of SiO and SiC (at 2.0 moles carbon)

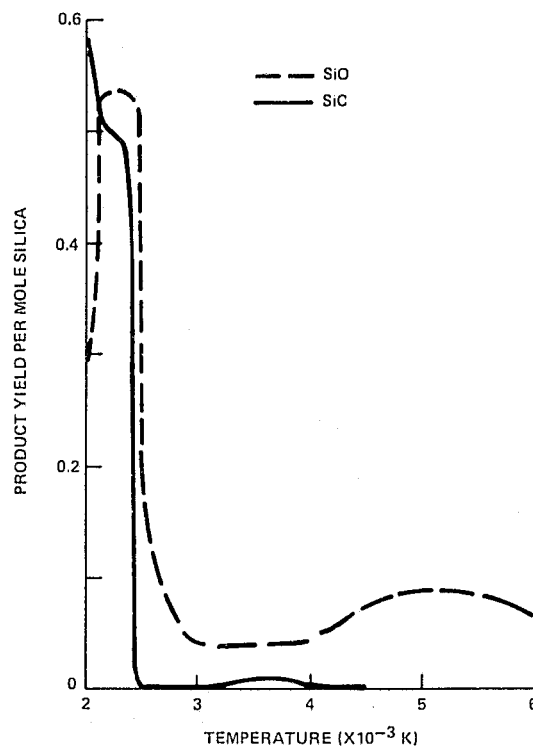


Figure 6. Reaction Products Below the Threshold Temperature

b. Heat Transfer Considerations

Achieving controlled temperatures near the minimum required to reduce silica is difficult due to the temperature gradient and the fluid characteristics within the plasma. The gradient ranges from 4000 K on the visible boundary to 16,000 K in the center with an overall average of approximately 6000 K.¹² The particles should be heated only to 2500 to 3000 K if the silicon is to be collected as a liquid. A suitable particle size must be selected for complete heating and reacting all of the material while vaporizing only a minimal amount. However, if the constraint of liquid silicon collection is removed and collection by condensing a gas is allowed, there is no upper limit to the temperature. This would seem to be advantageous since the reaction appears to increase its yield of silicon when all reactants are gaseous (>4500 K). Collection of the product by condensation of a gas is not as straightforward as the collection of a liquid and any impurities would not be the well-defined aggregates of slag in a liquid product.

The second consideration in heating solids particles is the fluid characteristics of the plasma. The particles lacking enough momentum to carry them through the surface of the plasma into the interior are deflected and travel only on the surface of the plasma, never being exposed to a sufficient amount of heat to initiate the reduction reaction. The relatively low density of silica and carbon particles aggravate the problem. If reactant forms other than silica and carbon are used, some of the above problems could be avoided. Silicon monoxide vapor and acetylene would react to form silicon in the cooler tail flame. The computer calculation predicts that silicon could be formed at temperatures as low as 1000 K. At higher temperatures (2000-3000 K), the silicon yield drops to zero. This decrease is due to the increase in silicon carbide formed by the decomposition of acetylene with subsequent recombination with reduced silicon monoxide.

3. Summary of Thermodynamic Analysis

A computational method for analysis of thermodynamics was extended to the silicon oxygen-carbon system. The reduction of silica to elemental silicon using carbon sources was considered and was thermodynamically possible. The optimum conditions for this reduction are a slight (2%) excess of carbon at a temperature between 2500 and 3000 K using silica and carbon black as reactants.¹³

B. MOLECULAR DYNAMICS OF PRODUCT QUENCHING

To have a usable silicon production process, quenching of the atomic species to a convenient and/or manageable temperature and extracting the product silicon are required. Thus, the goal of this study was to identify a quench rate that would maximize the production of silicon. Since the reaction to produce silicon in its elemental form has much less free energy than any side reaction, the minimization of the system free energy is identical with the maximization of the silicon production.

Molecular dynamics was used to model the quenching because the random nature of any collisions leading to reaction product other than silicon can be exploited to yield a close approximation to available experimental data. This technique was able to produce data in ranges of quenching rates where actual experimental data could not be obtained.

1. Computational Technique

Atoms of a given type, silicon, carbon, or oxygen, are randomly placed in a cube which has dimensions such that the density of the atoms is identical to that of these atoms in an experimental plasma. The cube dimensions are varied with respect to the sample size, from 100 to 500 atoms. The atoms are then assigned random velocities and directions. Atoms are then allowed to move in small time increments, normally on the order of 10^{-13} seconds. A constant density is maintained by requiring a new atom to enter the cell at the negative of the coordinate of the point from which an atom leaves the cell. For example, if an atom leaves the cube at (1, 1, 1), a new atom will enter the cell at ($\bar{1}$, $\bar{1}$, $\bar{1}$). The new atom has the same velocity vector as the atom leaving.

Interaction among the atoms is due to a hard sphere potential. The initial atomic temperature of at least 4000 K, the extremely fast quenching rate, and the low reactant atom density in the plasma contribute to the lack of any appreciable interaction among the reactant atoms. The major source of interaction is in the random collisions. When two atoms are within a given distance of each other, it is determined by the type of atoms and the temperature whether a reaction will occur. The primary thermodynamic consideration used in determining if the reaction occurs is that the Gibb's free energy is less than zero.

The total time elapsed in the calculations is approximately 0.5 ns in 5000 time increments. While this is a very short time span, it is consistent with that used by other investigators.^{14,15} Various initial configurations were used to determine if the products represented the equilibrium state of the system. The initial conditions used were 2.0 and 1.7 moles C/mole Si and 6000 K and 4000 K initial temperatures.

At the end of a calculation, the number of each of the products, Si, O, C, SiO, SiC, CO, and CO₂, were tallied. Also, the interatomic distance between each pair of atoms or molecules was punched into cards for later analysis.

2. Simulation Results

From the number and type of products formed in the quenching reaction, the free energy change from the atomic to the condensed state was calculated. These results are shown in Figure 7. There exists a free energy minimum which was found by fitting the parabolic portion of the free

energy curve to a second degree polynomial. Any error occurs in the choice of points to use in fitting the curve. Any of the five sets of points:

- 1) 1.7 moles C/mole Si, quenched to 600 K
- 2) 1.7 moles C/mole Si, quenched to 300 K
- 3) 2.0 moles C/mole Si, quenched to 600 K
- 4) 1.7 moles C/mole Si, quenched to either 600 or 300 K
- 5) All of the above points

will yield curves whose minima are within 2% of 4.56×10^{13} K/s. This minimum should occur where the maximum amount of silicon is found.

Data on silicon formation as a function of quenching rate is plotted in Figure 8. A maximum occurs at 4.66×10^{13} K/s. This figure is consistent with the free energy data plotted in Figure 7. The maximum amount of silicon formed is calculated to be 37% of all solids, Si, SiO, and SiC, present in the product.

Similar to the free energy curves, the major determinant of the amount of silicon production at quench rates higher than 10^{14} K/s is the final temperature. At such high quench rates, the material goes from the plasma temperature to the final temperature essentially instantaneously and equilibrates for the rest of the run at the final temperature.

These calculated results were compared with those found experimentally by determining the amount of silicon and silicon monoxide present in the condensate. The actual product as quenched from the plasma is an amorphous powder. This was sintered at 1500°C for one minute in an argon atmosphere to consolidate any silicon and to disproportionate much of the silicon monoxide. A quantitative analysis by wet chemical methods and qualitative analysis by x-ray diffraction were then done. Such disproportionation has been shown to convert 70% of the silicon monoxide to elemental silicon and silicon dioxide.¹⁶

Figure 9 shows the percentage of silicon calculated in the sintered product. There is no significant difference between the curves of material quenched to 600 K for either reactant composition. The major determinant of silicon content again appears to be the temperature to which the atoms are quenched.

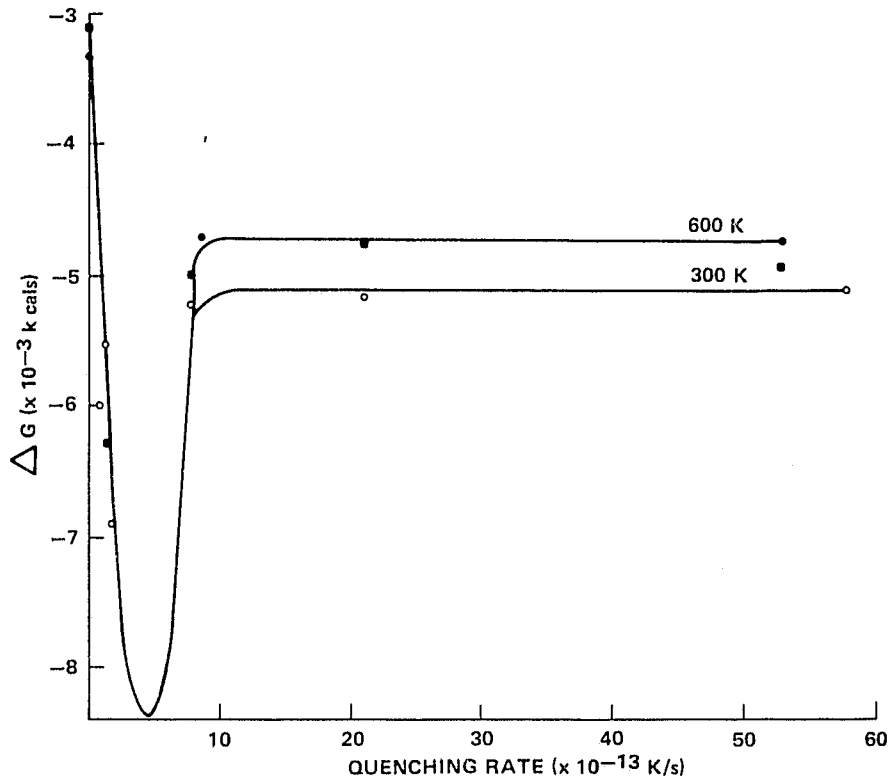


Figure 7. Free Energy Change Upon Quenching

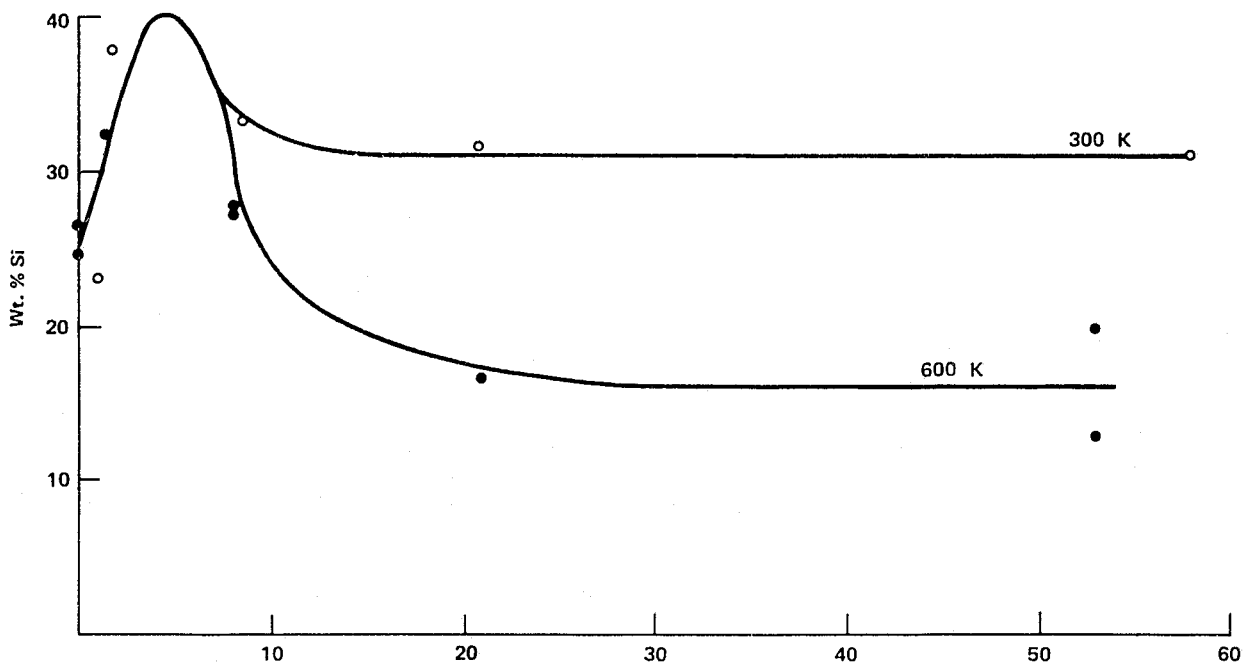


Figure 8. Formation of Silicon Upon Quenching

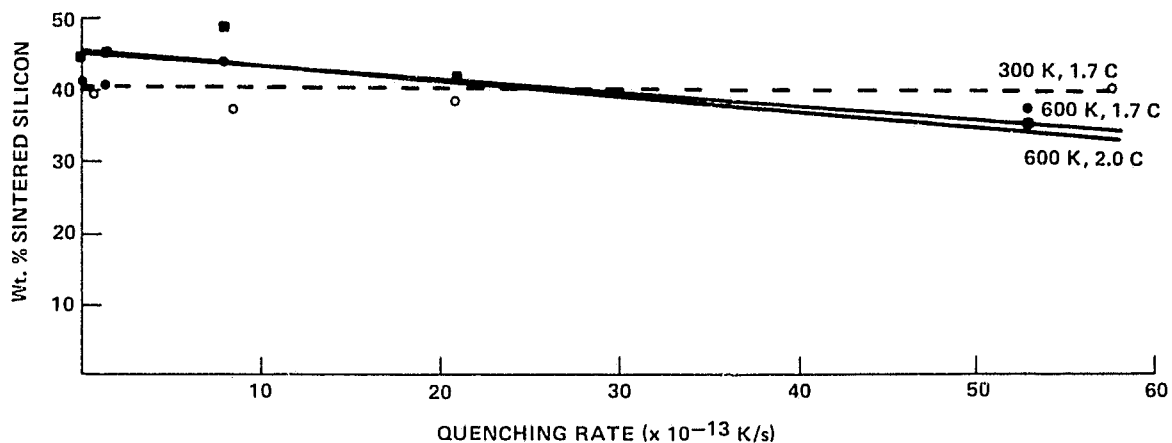


Figure 9. Amount of Sintered Silicon Upon Quenching

Experimentally, with 1.7 moles carbon per mole of silicon, analysis of the sintered product indicated values up to a maximum of 30% silicon when reactants were quenched onto a substrate estimated to be at 600 K. The 30% silicon content corresponds to a calculated quench rate that was faster than the rate estimated to occur in our experimental system. Therefore, it is suspected that either the analysis was slightly low or that the amount of disproportionation occurring was less than 70%. A quench rate of 1.05×10^{13} K/s, faster than estimated for the experiment, is also calculated to yield 30% of the product as silicon with no disproportionation. Since convection and position within the gas stream yield a range of quench rates to be expected in the experimental system, both silicon formation and disproportionation should occur.

The interatomic distance data is used in the Debye scattering equation to predict an x-ray diffraction pattern. The only recognizable feature of this pattern was the main beam and one broad peak from $k = 0$ to $k = 0.8$ where $k = 4 \pi \sin \theta / \lambda$. No definite peaks were calculated. Using standard techniques for x-ray diffraction of amorphous samples, a plot of the diffracted intensity versus k revealed no peaks other than the broad one as predicted. It was concluded from these data that the particles in the amorphous product are truly amorphous and very small (probably less than 100 Å).

3. Summary

The computer simulation technique of molecular dynamics was used to generate data on the formation of silicon as a condensate from a high-temperature plasma at various quench rates. These data show that there exists a maximum in the amount of silicon produced, but the quench rate indicated as being needed was beyond the experimental values and appears to be much too fast to be of practical utility.

Additional data was used to predict the x-ray diffraction pattern which should be observed. No major feature other than a broad central peak was predicted or observed. Such a peak is indicative of small particle sizes ($<100 \text{ \AA}$) and, consequently, highly amorphous material.

SECTION III TECHNICAL DISCUSSION

A. RAW MATERIAL SELECTION

Table 4 gives results of emission spectrographic analysis of several commercially produced carbon blacks and two high-purity silica flours. These materials were quoted in carload quantities to be \$0.25 to \$0.35 per kilogram for the carbon blacks and \$0.03 to \$0.07 per kilogram for the silica flour (400-mesh-grade material).

Appendices B and C are provided for additional information regarding detection limits.

Table 4. Emission Spectrographic Analysis of Raw Materials

	Carbon Black (ppm wt.)							Silica (ppm wt.)		
	Ashland 3023-P	Cabot BP-700	Cabot BP-1100	Cabot V-9A50	Huber N-110	RTV P-33	Detect. Limit	P G.S. Supersil	Wedron 400 M	Detect. Limit
Si	30-300	100-1000	100-1000	100-1000	30-300	30-300	0.08	Major	Major	--
B	ND	ND	ND	ND	ND	ND	0.08	10-100	1-10	0.15
Fe	30-300	10-100	30-300	100-1000	10-100	10-100	0.06	100-1000	30-300	0.25
Mg	10-100	100-1000	100-1000	10-100	10-100	1-10	0.006	10-100	10-100	0.0003
Mn	10-100	ND	ND	ND	ND	.1-1	0.02	10-100	0.5-5	0.07
Al	100-1000	100-1000	100-1000	30-300	.1-1	10-100	0.06	100-1000	30-300	0.2
Ti	1-10	3-30	3-30	3-30	ND	ND	0.08	100-1000	10-100	0.12
Ca	30-300	100-1000	100-1000	30-300	30-300	1-100	0.06	30-300	30-300	6.0
Cu	<1	<1	<1	<1	<1	<1	0.03	<1	<1	0.07
Na	>1000	100-1000	100-1000	100-1000	10-100	ND	0.05	10-100	3-30	4.0
Cr	ND	ND	3-30	ND	ND	ND	0.10	ND	1-10	2.5
Ni	ND	ND	1-10	ND	ND	ND	0.50	ND	ND	0.7
V	ND	ND	1-10	ND	ND	ND	0.06	ND	ND	1.1

B. LABORATORY PREPARATION OF RAW MATERIALS

The objective of the raw material preparation experiments was to optimize a procedure for achieving maximum intimacy of mixing and particle-to-particle contact. In light of the extremely short residence time ($\approx 10^{-2}$ seconds) in the plasma flame, it was important that the silica/carbon mixture be finely divided and homogeneous. The experiments simulated the condition of material processed in production-scale operations, such as a milling and spray drying.

Experiments with ball milling both dry and wet (aqueous slurry) confirmed the advantages expected of wet milling. It was found that the water content needed for dispersing the slurry from the mill was excessive and caused the larger and more dense silica particles to settle more rapidly than the carbon. Hence, segregation of the mixture resulted. A small addition, 0.5% by weight, of methyl cellulose (Dow Methocel) was made to the slurry to help prevent settling by increasing the viscosity and to act as a binder for increased strength of the dry "pelletized" material.

Photomicrographs of the silica/carbon (stoichiometric ratio of 1 mole SiO_2 to 2 moles C) mixture (Figure 10) show the result achieved by wet-milling on comminution and particle contact as compared with a dry blend of as-received materials. The SEM photograph shown in Figure 11 indicates the degree of silica and carbon particle contact of the minus 100 mesh mixture. The slurry was dried in a Teflon beaker on a hot plate while being stirred continuously. Final drying was accomplished in a forced-air oven set at $120^\circ \pm 10^\circ\text{C}$. The mixture was granulated by rubbing through a 35-mesh screen and finally screened to pass 100 mesh. This last step was known to be contaminating (the metal screen contacting the materials) but at this early stage of the work it was found expedient. Production batches would, of course, be spray-dried to a controlled distribution of pellet sizes.

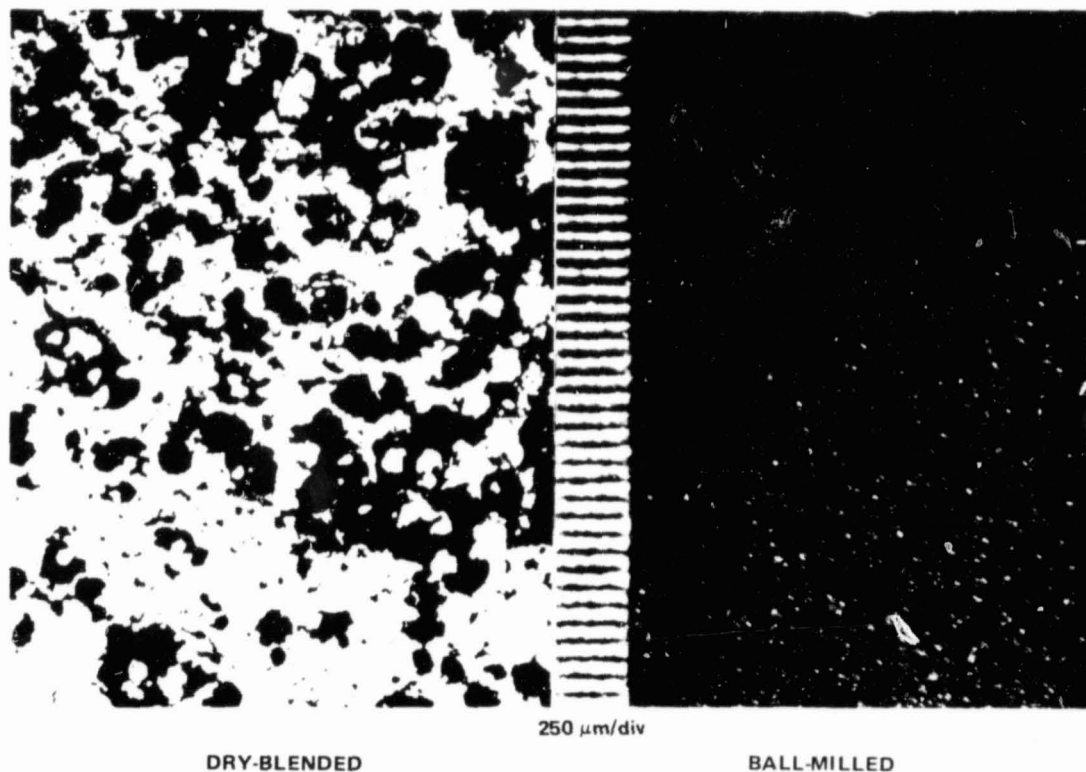


Figure 10. Silica/Carbon (2.5:1 wt ratio) Raw Material Mixture Photomicrograph



Figure 11. Carbon Particles Coating Silica (500X) – SEM

The batch weight and composition (stoichiometric ratio of 1 mole SiO_2 to 2 moles C) found suitable for laboratory studies was:

Silica	100 gms
Carbon Black	40 gms
Methocel	0.7 gm
Water	250 ml

Milling was for one hour with ≈ 1200 gms of flint pebble grinding balls. A screened fraction of the dried mixture between 35 mesh and 100 mesh, i.e., through the 35 mesh (420 micrometers) and retained on 100 mesh (149 micrometers), was apparently satisfactory from the standpoint of flowability of the powder.

C. RAW MATERIAL AND PREPARED BATCH ANALYSIS

Table 5 lists elements which were detected by emission spectroscopy in large (≈ 100 -lb) samples of raw materials which were received from the three carbon black producers and two silica sources. Table 6 shows the analyses of mixtures (SiO_2 -C, 2.5:1 ratio) prepared in the laboratory and by J. M. Huber Corporation. The experimental batches were ball-milled and pelletized. Of

Table 5. Emission Spectrographic Analysis of Raw Materials

	Carbon Black*, ppm wt				Silica**, ppm wt		
	Cabot V-9A50	Huber N-110	Ashland 3023-P	Detection Limit	PGS Supersil	Wedron 400M	Detection Limit
Si	100-1000	100-1000	100-1000	0.08	Major	Major	—
B	N.D.	N.D.	N.D.	0.08	10-100	10-100	0.15
Fe	30-300	10-100	30-300	0.06	100-1000	100-1000	0.25
Mg	1-10	3-30	3-30	0.006	1-10	10-100	0.0003
Mn	1-10	N.D.	1-10	0.02	1-10	1-10	0.07
Al	30-300	10-100	30-300	0.06	30-300	30-300	0.2
Ti	0.5-5	0.5-5	0.5-5	0.08	10-100	10-100	0.12
Ca	10-100	30-300	30-300	0.06	N.D.	N.D.	6.0
Cu	0.1-1	0.1-1	0.1-1	0.03	0.1-1	0.1-1	0.07
Na	100-1000	100-1000	100-1000	0.05	100-1000	100-1000	4.0
P	N.D.	N.D.	N.D.	1.0	N.D.	N.D.	1.0

* 50-lb sample

** 100-lb sample

Table 6. Emission Spectrographic Analysis of Mixtures (ppm wt)
Prepared in Laboratory and J. M. Huber Corporation

	C-4	C-5	B-4	H-2	C-6
Si	Major	Major	Major	Major	Major
B	10-100	10-100	1-10	1-10	3-30
Fe	300-3000	300-3000	100-1000	300-3000	100-1000
Mg	300-3000	300-3000	3-30	300-3000	30-300
Mn	10-100	10-100	1-10	10-100	1-10
Al	Minor	Minor	Minor	300-3000	300-3000
Ti	30-300	30-300	10-100	300-3000	30-300
Ca	Minor	Minor	10-100	Minor	100-1000
Cu	1-10	3-30	10-100	100-1000	0.1-1
Na	Minor	Minor	100-1000	Minor	100-1000
Be	<1	<1	N.D.	<1	<0.1
P	N.D.	N.D.	N.D.	N.D.	N.D.

Notes: Minor = 0.1 to 10%, all mixtures were SiO₂/C, 2.5:1 ratio by wt

Mix

Preparation Description

C-4 Large jar mill (≈5 liters) with flint pebbles, not screened

C-5 Small jar mill (≈1 liter) with alumina balls, not screened

B-4 Small jar mill (≈1 liter) with alumina balls, screened

H-2 Huber pelletized, Wedron SiO₂, screened

C-6 Milled in plastic container with flint pebbles, not screened

significance is the lower concentration of impurities, particularly Al, Ca, and Na, in material sampled from batch C-6. This batch was milled in a plastic container with flint pebbles in order to isolate the effect of contamination from the mill walls (usually alumina ceramic composition). In production operations rubber-lined mills would eliminate this source of contamination. The small amount of Cu, 0.1-1 ppm, in C-6 relative to the amount found in batches which were screened is also significant. It should be recognized that the impurities reported by emission spectroscopy are only semiquantitative.

D. PREPARATION OF RAW MATERIAL MIXTURES

1. Pelletized Batch for Pilot Scale Run

It was necessary to prepare a large (approximately 30 kg) batch of the SiO₂-C mixture for test runs to be carried out in the 350-kW IONARC furnace. The J. M. Huber Corporation at Borger, Texas, agreed to dry-mill and pelletize this material for Texas Instruments. Our laboratory experiments have used Huber's N-110 carbon black and Wedron's 400 M silica selected on the basis of highest purity as analyzed by emission spectroscopy.

The materials were dry milled and blended in a ball mill using flint pebbles and pelletized in a Turbulator or Pinnaixer. The pellets, though somewhat larger than desired, ranged in size from 250 to 1000 microns, Figure 12, and were extremely hard. The molasses binder, customarily used in pelletizing carbon black, imparted the necessary durability to the pellets for feeding to the plasma reactor. Distribution of pellet size was as follows:

Mesh Size	Batch, H-2	Micron Size
+20	8.5%	>850
-20, +35	90.4%	850-420
-35, +60	1.1%	420-250
-60	0%	<250

2. Material Preparation for Solid Feed Rod

An alternative approach to powder or pelletized feedstock was material formed into 6-mm diameter rods. A problem of friability of extruded rods was encountered initially in test runs using vendor's equipment. Binder additions improved the plasticity and strength of extruded rods. Five weight percent of polyvinyl alcohol (PVA), and sufficient water to produce good extrudibility were added to the ball-milled mixture and the binder imparted a high degree of dry strength to the material. The durability of the extruded rods was sufficient to withstand the heat exposure on entering the plasma flame without fracturing or decrepitating before being vaporized.

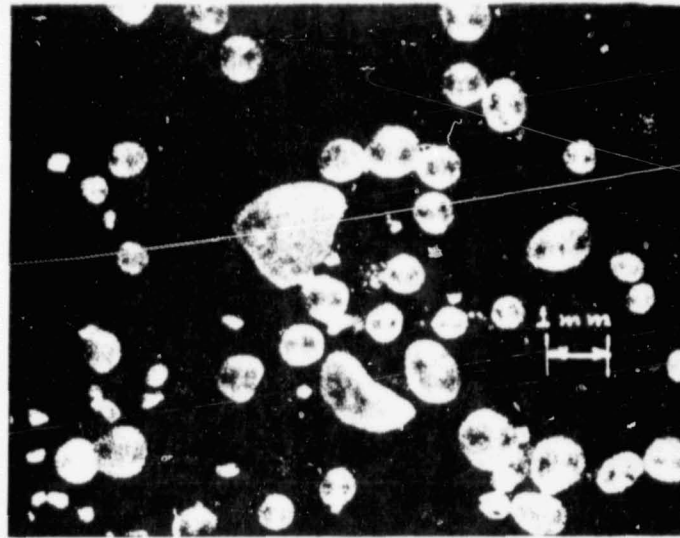


Figure 12. Pelletized $\text{SiO}_2\text{-C}$ Mixture

E. PLASMA TESTS USING VENDOR'S EQUIPMENT

Initially experiments on the plasma reaction were made with the aid of rented equipment: a small (10 kW), and intermediate-sized (40 kW) dc plasma torch, and a 350 kW pilot scale dc arc furnace. The feed systems for the equipment were limited and a certain degree of improvising was necessary. The large system was restricted to feeding raw material of a specific pellet size distribution. The vendor's facility was used in an attempt to accomplish the following:

- 1) Verify that SiO_2 can be reduced to silicon with carbon in an argon plasma
- 2) Demonstrate the feasibility of feeding a solid rod of the SiO_2/C mixture to the plasma and compare with feeding pelletized material
- 3) Compare the operation of an RF plasma with a 40 kW dc device
- 4) Collect the product on a fused silica probe as well as on a water-cooled copper tube wall
- 5) Test silicon addition to the SiO_2/C mixture to investigate a liquid phase reaction
- 6) Evaluate a pilot plant size (350 kW) dc arc furnace.

1. Material Preparation for IONARC Furnace Test

Plasma tests at TAFE/Ionarc* were made with raw material of increased pellet strength and durability. This property and a closely controlled pellet size (between 150 and 500 microns) were specified for the test of the IONARC furnace (Figure 13). Hard pellets were necessary since the feed mechanism of the large reactor was mechanically abusive to the pellets and would break friable pellet. The fine powder material would not penetrate the plasma flame but was merely deflected away much as a column of water would deflect a less dense substance. The advantages of this IONARC furnace were the longer residence time (the flame is about 6 feet long) and better opportunity for quenching and collecting the product under controlled atmospheric conditions.

Preparation of a 30 kg sample of pelletized mixture of very hard pellets and close size range for the proposed IONARC furnace test was done by J. M. Huber Corporation at Borger, Texas.

2. IONARC Furnace Tests

Eight test runs were made in the 350-kW plasma reactor. The material processed was the stoichiometric ratio of one mole of silica to two moles of carbon, or SiO_2/C weight ratio of 2.5:1.0. Pellet sizes ranged between 250 and 1000 microns.

Two of the variables in the IONARC furnace tests were vacuum in the chamber and number of air entrance ports open. The ports were located on top of the furnace cylinder. The vacuum maintained within the chamber determined the velocity of the air flowing and the number of open ports controlled the volume. With these parameters it is possible to partially control the oxidizing or reducing atmospheric conditions within the furnace. The injection nozzle angle could only be varied by changing the headpiece of the furnace feed mechanism. Three nozzles were used for the tests. A larger angle (29 degrees) injection nozzle should have provided greater penetration of material into the plasma flame. The angle is measured with reference to the flow direction of gas in the chamber, the greater the angle, the more nearly normal or perpendicular to the flow.

The collection unit was a water-cooled conical shaped sheet of copper about 12 inches in diameter at the top. Distance of this collector was about 30 inches below the carbon arc rods, i.e., well within the range of the plasma flame and thus subject to high temperatures. Survival of the copper collector was in question during the experimental runs, D-7 and D-8.

*TAFE Div. of Ionarc Inc., Bow, New Hampshire

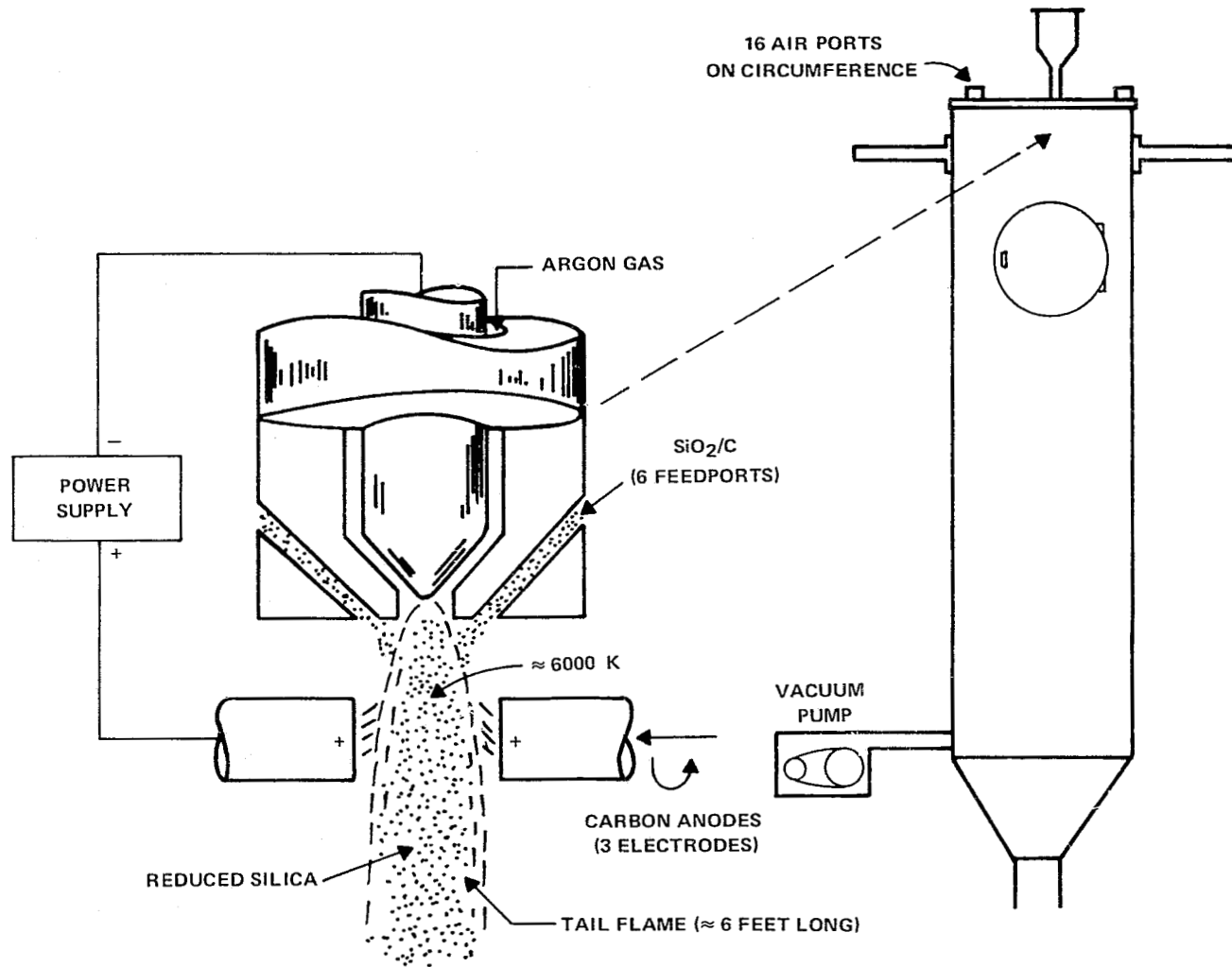


Figure 13. 350-Kilowatt IONARC DC Plasma Furnace

Feed rate of the pelletized material was held constant at 60-lbs per hour except for the first and last runs and carrier gas was either Ar or N₂. Time for a run was varied between 2.5 and 10 minutes but this is not considered significant to the results obtained.

A summary of IONARC furnace tests, runs D-1 through D-8, may be seen in Table 7. The appearance of product formed from each test run is indicated in the last column.

Table 7. IONARC Furnace Tests

Run No.	Power (kW)	Vacuum in Chamber (in H ₂ O)	Run Time (min)	No. Ports Open to Atmos.	Carrier Gas	Injection Nozzle Angle (degrees)	Appearance
D-1	276	10	2.5	6 at top	Ar	23	Fumed SiO ₂ , C
D-2	276	10	2.5	6 at top	N ₂	23	Fumed SiO ₂ , C
D-3	231	1.5-2.0	8	0	Ar	23	SiO _x , SiC
D-4	231	2	3	3 along carbon rods	Ar	23	SiO _x ,* SiC
D-5	231	1.5-2.0	3	3 at top	Ar	29	SiO _x ,* SiC
D-6	276	7	3	6 at top	N ₂	26	SiO _x , SiO ₂
D-7**	276	9-10	10	6 at top	N ₂	26	Fumed SiO ₂ , SiO _x
D-8**	346	9-10	5½	3 at top	N ₂	26	SiO _x ,* Fumed SiO ₂ , SiC

All tests used argon as arc gas and ran for 5 minutes prior to injection of powder.

- Notes:
- Six ports open with 10 inches H₂O (Vac.) equivalent to 800 SCFH air
Argon flow rate was approximately 150 SCFH
 - Powder flow rate was 60-lbs/hr for all runs excepting D-1 (119-lbs/hr) and D-8 (150-lbs/hr)
- * Good reaction (N₂O₄ evolved) with HF/HNO₃
- ** Catch unit used on runs D-7 and D-8

In general, the product formed in the IONARC furnace reaction indicated insufficient residence time for pellets to reach the desired temperature. The major portion of material which passed through the reactor chamber seemed not to penetrate the flame, hence was unreacted silica and carbon. A large percentage was also silicon monoxide or SiO_x and SiC. Because of the masking effect of the unreacted silica, x-ray diffraction indicated α quartz only. SiO does not give a clearly defined diffraction pattern, hence is not identifiable on the Debye-Scherrer photograph.

One explanation for the incomplete reaction observed from these test runs relates to the plasma flame temperature profile. As described under the thermodynamic analysis of the reaction, there is a threshold temperature which must be reached for the reaction to occur that will yield silicon. The inner core of the IONARC furnace Ar plasma flame was estimated to be around 6000 K. The temperature drops off from the highest point (6000 K) in the ≈8-inch diameter flame

in a Gaussian distribution. It is questionable that the majority of pellets ever reached the inner portion of the flame or, if so, would have had sufficient residence time for the larger (>250 microns) pellets to reach the necessary threshold temperature.

The fact that some of the silica was reduced to SiO_x (where x is <2.0) was verified by an acid test. HF/HNO_3 etchant produces a visible reaction which evolves brown-colored vapors of N_2O_4 . Silica, as quartz, does not react with the HF/HNO_3 mixture to evolve nitrous oxide.

The large amount of fumed silica in the reaction product was due to the partially oxidizing atmosphere which existed within the cooling portion of the reaction chamber — a condition which was impossible to control with the present furnace design. It is felt that much of the reduced silica, whether as Si or SiO_x , was reoxidized as it cooled, or was quenched, from the elevated reaction temperatures.

3. DC Torch Tests

A 40-kW dc plasma torch with a reaction and quenching chamber attached directly to the torch nozzle was used for additional test runs. One test was also made on a small RF unit using Ar as plasma gas. The material (SiO_2 -C mixture) was in the form of dry-pressed pellets 1-inch diameter by approximately 1-inch length or ½-inch diameter rods about 3 inches long. The pellets or compacts had holes drilled axially through their centers to the approximate diameter of the torch exit nozzle. The rod shapes were exposed to the plasma flame as solid pieces.

Table 8 summarizes the 40-kW dc torch test runs. Limited analytical results are also reported in Table 9 for material produced in these and IONARC furnace tests.

The reaction product condensed on the walls of the water-cooled copper tube immediately downstream from the impingement of the plasma flame on the solid compacts. Runs K-6, K-7, and K-8 are examples. Run K-6 condensate was identified by x-ray diffraction analysis as principally elemental silicon with SiO_2 and SiC present. If SiO_x were present, it would not have been obvious from the x-ray pattern. This particular test run, K-6, used H_2 as a carrier gas. The H_2 gas was introduced at the point where powder would normally be fed to the torch but in this case no powdered material was used. The H_2 assured a nonoxidizing or reducing ambient during the reaction and during quenching or cool down. It must be concluded that the H_2 as a carrier gas (or possibly as the arc gas) will be beneficial to plasma reduction reaction.

Table 8. Experiments Using DC and RF Torch

Run No.	Arc, Type	Carrier Gas	SiO ₂ -C Form	Time (s)	Appearance of Specimen	Analytical Results
K-1	dc,	Ar/Propane	Pressed Pellet	10	Metallic luster, nodular hard section from I.D. of pellet	X-ray indicates α quartz and minor amount of SiC. Pyrolytic carbon is also present.
K-2	dc,	Ar	Pressed Pellet	10	Gray, hard, porous crust formed on I.D. of pellet	No reaction with HF/HNO ₃
K-3	dc	Ar	Pressed Pellet	30	Same as K-2	No reaction with HF/HNO ₃
K-4	rf	Ar	Rod	30	Gray-green, soft residue on tip of rod	Probably SiO _x coating unreacted SiO ₂ -C. SiC also present
K-5	dc	H ₂	Rod	30	Gray, brittle residue on surface of rod	Slight reaction with HF/HNO ₃
K-6	dc	H ₂	Pressed Pellet	30	Yellow-brown, soft deposit from water-cooled tube	Probably SiO _x . Si, SiO ₂ and SiC from x-ray. HF/HNO ₃ reaction
K-7	dc	Ar	Pressed Pellet	30	Gray, soft powder collected in water-cooled tube	Probably SiO _x . SiO ₂ , SiC, and possibly Si from x-ray. HF/HNO ₃ reaction
K-8	dc	CH ₄	Pressed Pellet	30	Gray, hard powder collected in water-cooled tube	Unreacted carbon and condensed SiO _x . No HF/HNO ₃ reaction

Notes: 1. SiO_x, where $x < 2$
 2. All tests used Ar as arc gas.

Table 9. Analytical Results of Reaction Product from Plasma Tests

IONARC Furnace Run Samples	HF/HNO ₃ Reaction (N ₂ O ₄ Evolution)	Detected by X-Ray Diffraction
D-2 Bottom	Slightly visible	SiO ₂
D-2 Wall	Slightly visible	SiO ₂
D-4 Wall	Significant	Amorphous SiO ₂
D-5 Wall	Significant	SiO ₂
D-8 Wall	Readily visible	
D-8 Cone	Significant	SiO ₂
D-8 Cone (Oxidized HF etched)	—	SiC
D-8 ID of Cone	Significant	SiO ₂
DC Torch Run Samples		
K-1	None	SiO ₂ , SiC
K-6 (Condensate)	Significant	Si, SiO ₂ , SiC
K-7 (Condensate)	Readily visible	SiO ₂ , possibly Si, SiC

Note: Reaction with HF/HNO₃ (50/50) with the evolution of brown vapors of N₂O₄ indicates that the product contains reduced silica as SiO_x (where x < 2) or elemental silicon.

4. Results of Additional Tests

The powder feed runs were encouraging in that the product apparently contained material which reacted with HF/HNO₃ indicating the silica had been partially reduced. This was the first success with feeding powder to the small 40 kW dc torch. Feeding the 1/8-inch diameter rod material caused the rods to quickly disintegrate. Large portions of the unreacted rod were simply carried away from the hot zone. See Figure 14 for an illustration of the experimental setup for the 40 kW dc torch runs using the feed rod approach. The friability of extruded rods was subsequently solved, as discussed previously, by the addition of PVA as a binder.

Feeding the 6-mm diameter rod material into the RF unit (from an opening on top of the torch housing) was also unsuccessful because the rods could not be held satisfactorily in position long enough to reach the high-temperature zone in the plasma flame.

Analytical results of the reaction products from these additional test runs are in Table 10. X-ray diffraction was used to identify the crystalline components present in the material and a wet chemical technique in combination with colorimetric comparison was used to determine the amount of silicon present (Appendix D). Silicon was detected in run 4, sample 4B which was

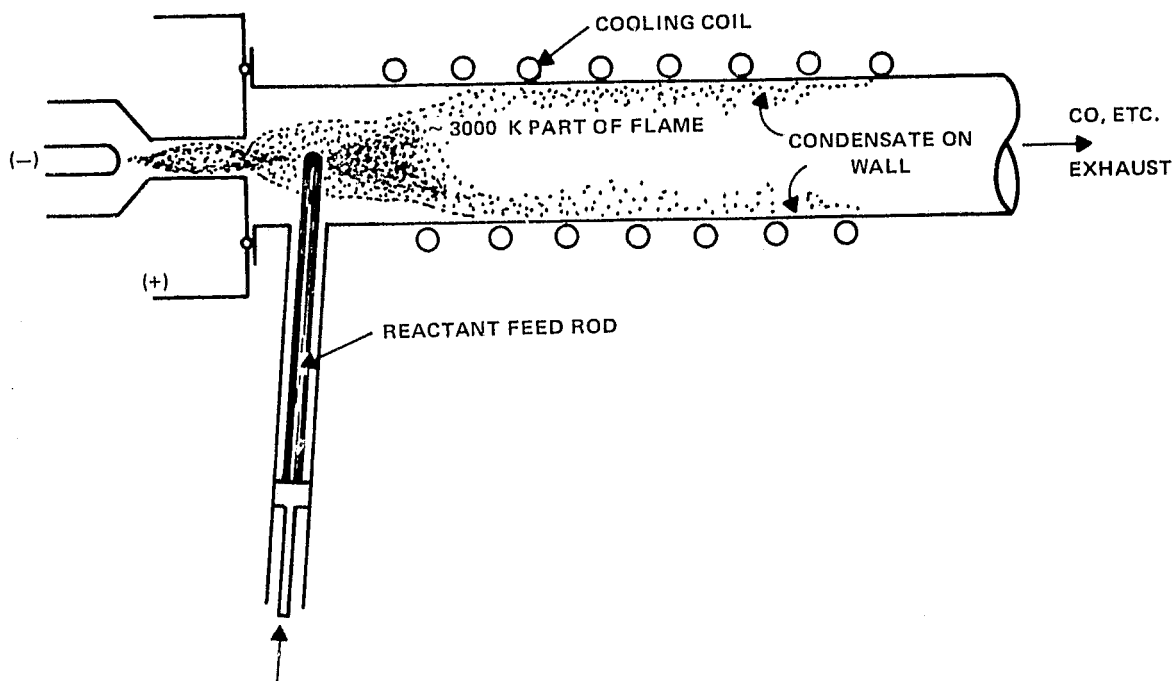


Figure 14. DC Plasma Experimental Setup for Solid Feed Rod

Table 10. Analytical Results of Reaction Products

Run No.	Feed Material Mix	Form	HF/HNO ₃ Reaction	Detected by X-ray	Wet Analysis Colorimetric Silicon Content
2	C-2	Powder -60 mesh	None	amorphous	
3	C-2	Powder -60 mesh	Slightly visible	SiO ₂	
4A	C-2	Powder -60 mesh	None	SiO ₂	
4B	C-2	Powder -60 mesh	Slightly visible	SiO ₂ , Si	
4C	C-2	Powder -60 mesh	Significant	SiO ₂	≈0.5%
5	C-2	1/8 inch rod	Significant	SiO ₂	≈0.5%
6	C-2	1/8 inch rod	Significant	SiO ₂ , Si	≈2.0%
7A	B-6	1/8 inch rod	Readily visible	SiO ₂ , Si	
7B	B-6	1/8 inch rod	Readily visible	SiO ₂ , Si	≈3.5%
8	C-2	1/4 inch rod	None	SiO ₂	
12	C-2	Powder -60 mesh	None	SiO ₂	
13	C-2	Powder -60 mesh	None	SiO ₂	

NOTE: C-2 was stoichiometric mixture of SiO₂ and C
B-6 had 30% silicon added to mixture

obtained from the silica plate covering the cooled copper tube. Run 4 was a powder-fed run. This was the first indication that it was possible to react material fed to the plasma in a pelletized form to a degree sufficient for silica to be reduced to elemental silicon. Amount of silicon, approximately 3% in the product collected, was extremely low however.

F. DESIGN AND FABRICATION OF EXPERIMENTAL REACTOR

1. Experimental Reactor Description

An induction heating system unit was used to construct an RF plasma reactor. A two-turn coil around a 30-mm diameter quartz tube had provisions for introducing and measuring the arc, sheath, and carrier gases as shown diagrammatically in Figure 15. The sheath gas acts as a cooling or insulating shield between the hot plasma flame and the quartz tube wall. Carrier gas transports the powder (pelletized material) into the plasma flame. The 30-mm flame containing tubing expands into a larger 75-mm quartz tube which contains the quenching/cooling system.

The initial quenching arrangement was an air-cooled quartz plate located approximately 20 cm from the center of the plasma flame. The gases from the flame and gaseous products formed are

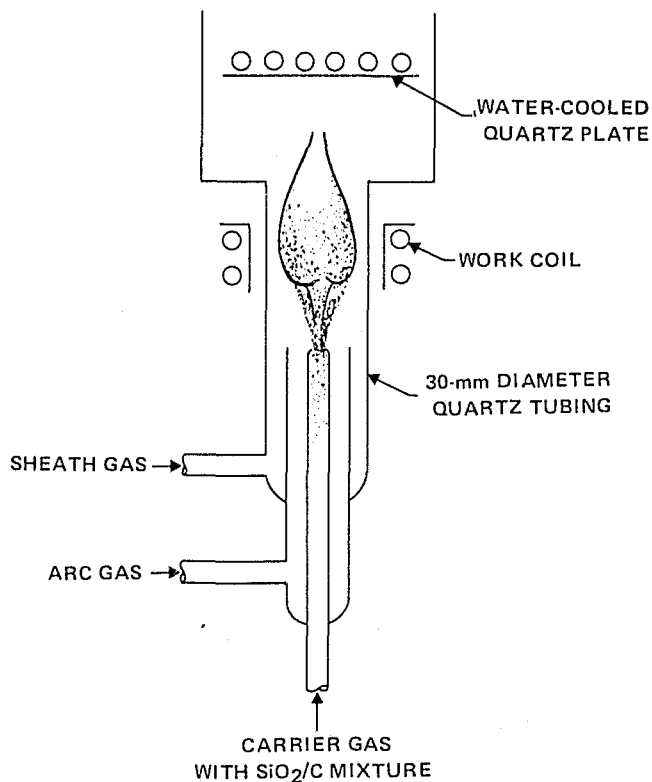


Figure 15. Experimental RF Plasma Reactor

exhausted in a semienclosed manner such that ambient air is excluded from the quenching region. The initial raw material feed mechanism was an electrically driven auger which fed powder into the gas stream. Rods (≈ 6 mm diameter) were fed from the tube which feeds the powder and carrier gas.

2. Reactor Design Modifications

In the original design it was observed that the plasma flame was skewed off the axis of the fused silica tube. Often, the tube would develop a hole after about 10-minutes operation from localized melting of the tube wall where the flame was in close proximity. Published data on RF plasma torches¹⁷ stated that when the discharge is vortex-stabilized it can be maintained on the axis of the tube even if the diameter of the flame (in our case about 1.5 cm) was much greater than the skin depth of the plasma gas. To provide this axial symmetry, the sheath gas which cools the tube wall was introduced tangentially into the tube instead of radially as in the original design. This corrected the off-axis problem and significantly stabilized and extended the flame length (from ≈ 3 cm to ≈ 10 cm) (Figure 16).

The efficiency of collecting product from the SiO_2/C reaction depends mainly on how effectively the silicon vapors can be quenched, i.e., by rapid heat transfer onto a cool surface, such

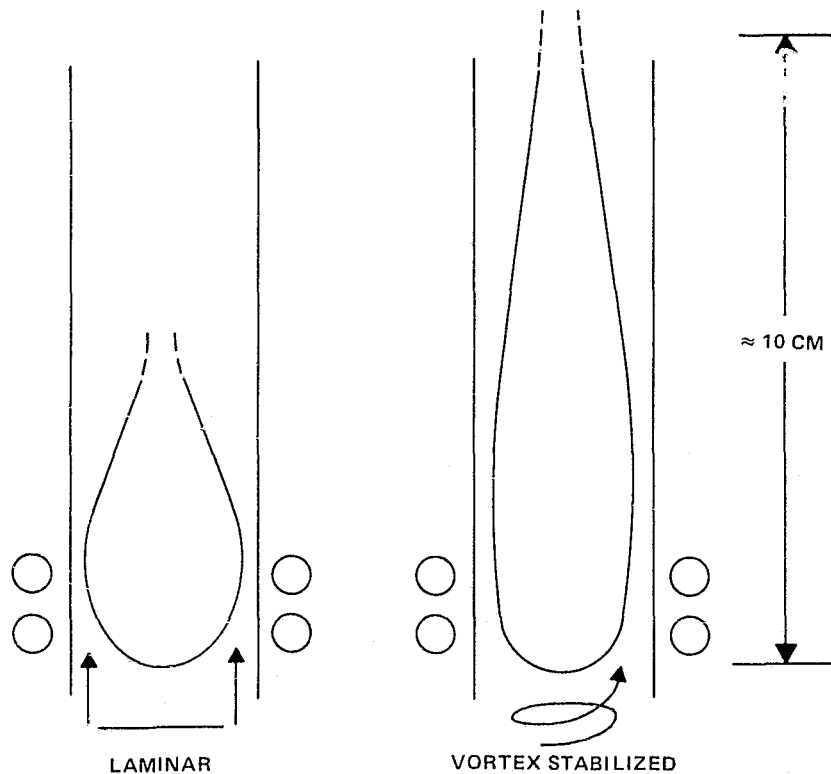


Figure 16. Effect of Sheath Gas Flow on Plasma Flame

that the vapors can be condensed without becoming reoxidized. It was apparent that in the initial quenching system, an air-cooled quartz plate inside of the cooling portion of the reactor, was not sufficiently effective. To improve the quench rate, a water-cooled copper tube was used to cool the plate or baffle and the tube wall. This improved the quenching but did not aid collecting product to any significant degree.

An improved version of the experimental induction plasma reactor was fabricated. Figure 17 is a diagram of the assembly of fused-silica tubing with O-ring seals and the water-cooled jacket. The system was much easier to disassemble for cleaning between runs and less complicated than the original one-piece reactor with fixed fused-silica appendages. Repositioning the relative heights of the arc and carrier gas tubes was possible. Figure 18 is a reactor system showing quenching tube (top), powder feed setup (bottom) and gas and power controls. Another modification provided water-cooling for the jacket and a water-cooled metal flange with O-ring seals for coupling the nozzle tube to the quench chamber.

The auger-type powder feeder which worked satisfactorily with pelletized material did not function with the fine ($<37 \mu\text{m}$) silica powder. The poor flow characteristics of the material, due to the size and shape of the particles, did not allow a continuous feed rate to be achieved. The system

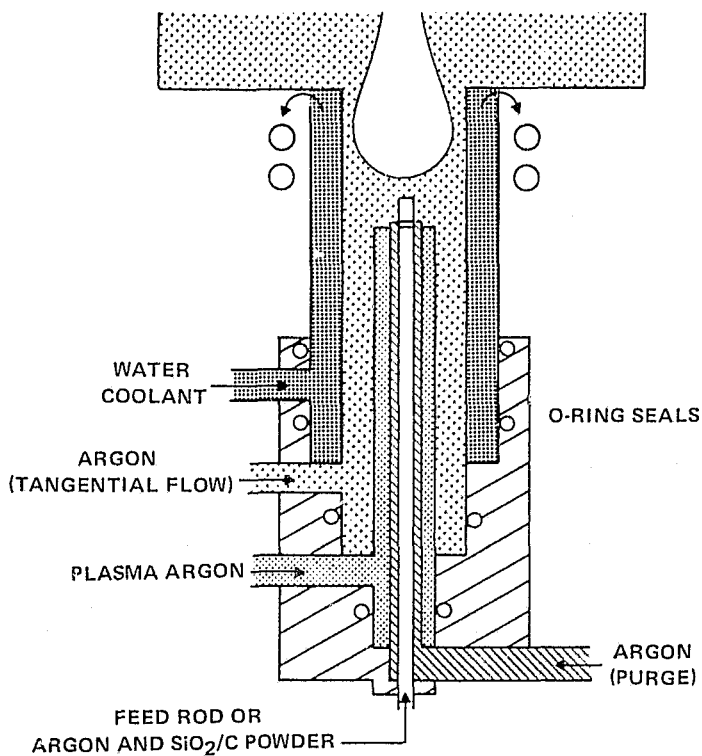


Figure 17. Improved Design of Induction Plasma Reactor

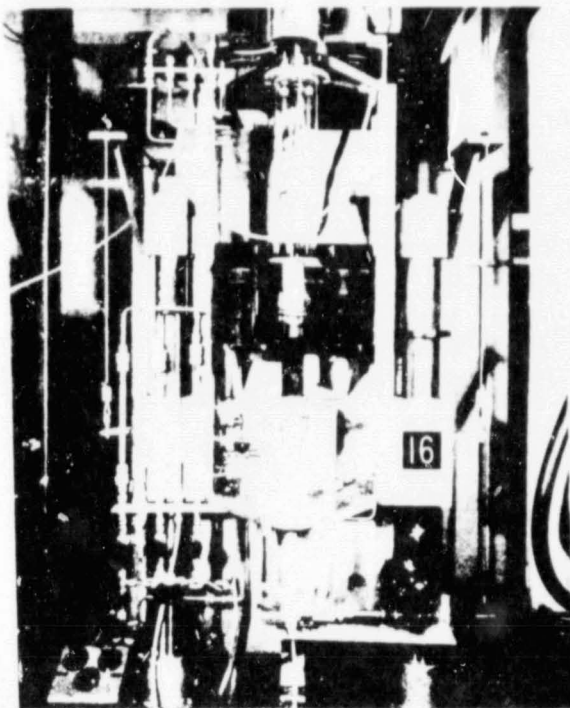


Figure 18. Experimental Induction Plasma Reactor

was modified to force gas up through the powder and suspend the particles allowing material to be conveyed up into the carrier-gas tube. The feed rate was extremely low and the setup was found to be unsatisfactory for feeding the finely milled powder.

A mechanism was constructed for continuously feeding a rod of the raw materials to the plasma flame. The feed rate was controlled by a variable speed motor which drove a threaded rod, which in turn moved the feed rod vertically into the reaction chamber.

A tubular bundle was fabricated to act as a surface for cooling the hot gases and positioned within the quench chamber such that the product could be collected at an elevated ($>400^{\circ}\text{C}$) temperature. This modification in the collecting system was decided upon after evaluating a water-cooled probe and after experimentation with heating the cooling chamber wall for determination of an optimum temperature for quenching. Other alternatives to collecting (condensing) the reaction product which were tried will be discussed in subsequent sections.

3. Flame Temperature Mapping

The temperature profile was determined by measuring and comparing the relative atomic spectral line intensities. Argon lines at 7635, 7514, 7384, and 7724 Å were used. The experimental setup is depicted in Figure 19. The emitted radiation from the plasma is passed through a Jarrell-Ash 0.25 meter Ebert monochromator where these lines are extracted. The intensity of the subsequent radiation of a single wavelength is measured using a Princeton Applied Research Corporation quantum photometer equipped with a Hamamatsu R636 photomultiplier tube. These intensities are then converted to temperature profiles using the inverted Abel integral equation

$$i(r) = \frac{-1}{\pi} \int_r^R \frac{I'(x) dx}{(x^2 - r^2)^{1/2}} \quad (1)$$

where

$i(r)$ = radial intensity function at level Z

$I'(x)$ = first derivative with respect to x of the measured intensity along a chord of the cylindrical plasma at level Z

R = radius of the plasma

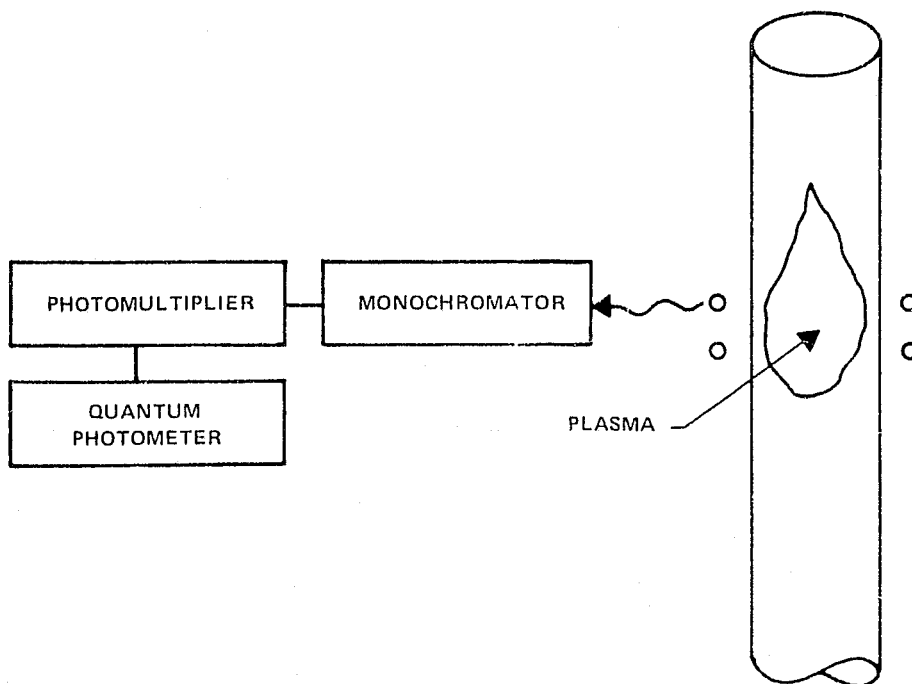


Figure 19. Equipment Diagram for Temperature Measurement

The difficulty in using this equation was a magnification of the noise in the data when the derivative of $I(x)$ is evaluated. In addition, the numerics tend to be unstable in the center, the region of greatest interest, and lend undue weight to the outer fringes where the measurements are relatively uncertain. There is an advantage to reversing the order of differentiation and integration and to apply the smoothing techniques after integration, but before differentiation.^{18,19} It can be shown that

$$i(r) = -\frac{1}{\pi r} \frac{d}{dr} \int_r^R \frac{I(x) x dx}{(x^2 - r^2)^{1/2}} \quad (2)$$

where

$i(r)$ = radial intensity function at level Z

$I(x)$ = the measured intensity along a chord of the plasma at level Z

R = radius of the plasma

Equation (2) can be written as

$$i(r) = -\frac{1}{2\pi r} \frac{dF(r)}{dr} \quad (3)$$

where

$$F(r) = 2 \int_r^R \frac{I(x) x dx}{(x^2 - r^2)^{1/2}} \quad (4)$$

The experimental data are fitted by least squares to a function $I(x)$ that is analytically integrable in equation (4) so that once the curve fitting is accomplished the solution may be written down immediately. The functional form used is

$$I(x) = \sum_i C_i (R^2 - x^2)^i \quad (5)$$

where the constants C_i are to be determined. Adequate accuracy has been found using six terms. The solution is then:

$$F(r) = \sum_i C_i (R^2 - r^2)^{i - 1/2} \quad (6)$$

where

$$\lambda_i = [\Gamma(i+1)/\Gamma(1/2)\Gamma(i+1/2)]$$

or, more convenient computationally,

$$\lambda_i = (2^{2i}/\pi) [(i!)^2/(2i)!] \quad (7)$$

The exact numerical procedure involves fitting the experimental data to a function that assures the C_i may be a linear function of x in order to take any antisymmetries of the intensity distribution into account as:

$$I(x) = \sum_i (a_i + b_i x) (R^2 - r^2)^i \quad (8)$$

This gives the symmetrical solution of $F(r)$

$$F^+(r) = \sum_i \lambda_i a_i (R^2 - r^2)^{i-1/2} \quad (9)$$

and the antisymmetric solution

$$F^-(r) = \sum_i \lambda_i b_i r (R^2 - r^2)^{i-1/2} \quad (10)$$

The computations use the intensity measurements from 14 positions within the plasma inserted into equation (8). An intensity of zero is assumed at the edge of the plasma. These linear equations are then solved simultaneously by a least squares method for the coefficients a_i and b_i which are used in equations (9) and (10). The sum of equations (9) and (10) gives the expected intensity at a particular radius.

These temperature profiles are found by taking the ratio of the ionic and atomic lines or argon. This assumes that the partition function and the number of particles are constant or, at worst, weak functions of temperature and that the relative transition probabilities are known. With this information, an intensity ratio may be derived from the Saha equation:

$$\frac{I_1}{I_2} = \frac{g_m^1 A_n^m v_1}{g_m^2 A_n^m v_2} \exp \left[\frac{-E_{m1} + E_{m2}}{kT} \right]$$

where

I_1 and I_2 = intensities of the atomic and ionic lines

g_{m1}^1 and g_{m2}^2 = statistical weights of the atomic and ionic states

A_n^m = spontaneous transition probabilities from state 1 to 2

ν_1 and ν_2 = frequencies

E_{m1} and E_{m2} = the energies of the atomic and ionic lines

k = Boltzmann's constant

T = absolute temperature

This equation may be solved directly for T or a graph of $\log(I_1/I_2)$ versus $-(E_{m1} - E_{m2})$ may be plotted. The graph should be a straight line of intercept $\log(g_{m1}^1 A_n^m \nu_1 / g_{m2}^2 A_n^m \nu_2)$ and a slope of $1/T$.

The radial intensities were calculated from measurements at four wavelengths, and all possible ratios among them were calculated. The linear least squares regression of these ratios versus the difference in energy states gives an accurate description of the temperature profile. These temperatures are generated across one level and compound with those of others yielding the profile in Figure 20. Note that the highest temperature portion of the plasma ($>10,000$ K) is only a very small area, while the region which is greater than 5000 K is large enough to be easily used as a target for the rod feed. This will ensure the heating of the SiO_2/C mixture to temperatures greater than the vaporization point of each component.

G. EXPERIMENTAL PLASMA REACTOR TESTS

1. Scoping Experiments

The initial experiments (Table 11) with the reactor fed powdered raw material (SiO_2/C , 2.5:1 wt ratio) to the flame. Difficulty with feeding the powder at a constant and sufficiently low rate was experienced. Feeding solid rods of extruded material into the flame was more successful. The vaporization of material from the rod was more easily controlled and the residence time appeared to be sufficient for complete reaction when feed rates were in the order of 0.02 to 0.10 gm per minute. With an excessive rate of insertion of the rod into the flame, even though the material appeared to completely vaporize, the raw materials were incompletely reacted.

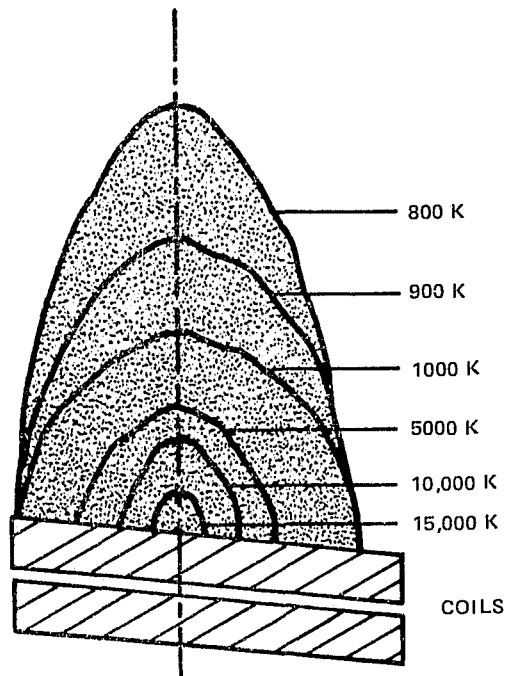


Figure 20. Temperature Profile of Plasma Flame

When an extruded rod made with the silica containing a 10% PVA binder addition was fed, the silica vaporized and dissociated as evidenced by the light brown powder (condensate) collected on quenching. This experiment raises questions about the optimum amount of, and/or the effectiveness of the carbon form in reducing the silica to elemental silicon. The extremely high-temperature argon plasma apparently possessed sufficient energy to partially decompose the oxide into silicon and oxygen.

a. Methane Experiment (Gaseous Form of Carbon)

When SiO_2 in extruded rod form (with PVA binder) and CH_4 were introduced into the plasma arc, the flame brightness increased significantly and the tail flame extended far into the quenching chamber. Control on the CH_4 flow rate was not precise and an excess of carbon was present during the reaction. The product appeared to be mostly unreacted carbon, but microscopic beads of silicon were visible at 70X magnification. A precision flowmeter and micrometer control valve were installed on the system to control the CH_4 at the milliliter per minute range stoichiometrically equal to the ≈ 0.05 gm/min SiO_2 feed rate. The run was repeated with CH_4 controlled to about 4 ml/min while feeding ≈ 0.03 gm/min of a 3-mm diameter rod [composed of SiO_2 (-400 M) with 5% PVA added as a binder]. Results were more satisfactory. The product collected was a brown-black colored condensate but appeared to contain a significant amount of unreacted carbon.

Table 11. Scoping Experiments with Induction Plasma Reactor
(Raw Material Form and Feed-Rate Experiments)

Run No.	Gas Arc	Flow Sheath	l/min Carrier	Amps	Volts (kV)	Powder	Material Feed Rod (6mm dia)	gms/min	Comments
P-1	2	15	2	2.3	5	B-4 -60M		>0.5	Uncontrolled feed rate. SiO ₂ partially reduced.
P-2	2	15	2	2.3	5	B-4 -100M		>0.5	Uncontrolled feed rate.
P-3	2	15	2	2.3	5	B-4 -100M		≈5	Excessive feed rate. Unreacted.
P-4	2	15	2	2.3	5	B-4		0.5+5	Variable feed rate. Partially reacted.
P-5	2	15	1	2.3	5		C-2	≈0.2	Epoxy-coated rod. Mostly reacted.
P-6	2	15	1	2.3	5		C-2	≈0.2	Vortex stabilized flame. Material was vaporized and reacted
P-7	2	15	1	2.3	5		SiO ₂	≈0.2	SiO ₂ completely vaporized. Partially reduced.
P-8	2	15	1	2.3	5		Si	≈0.2	Collected vaporized Si as a brown-colored powder.
P-9	2	15	1	2.3	5	B-4 -100M		<0.5	Vortex stabilized. Material did not penetrate the flame.
P-10	2	15	1	2.3	5		C-2	≈.08	Material vaporized more slowly. Flame penetration was difficult.

B-4 powder, 2.5:1 (SiO₂ : C) by wt with Methocel

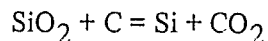
C-2 rod, 2.5:1 (SiO₂ : C) by wt with PVA

SiO₂ and Si rods were powdered material with PVA binder

The results of the tests using methane carbon source suggested the possibility of using other hydrocarbons as reactant feedstock. For example, the petroleum base stock (a by-product from the refinement of crude oil) now used to produce carbon black could be vaporized and fed directly into the plasma flame instead of using solid carbon.

b. Reduced Carbon Content in Mixture

Test runs were conducted with feed rods composed of silica/carbon mixture with a mole ratio of 1:1 as compared to the original stoichiometric mixture of 1:2 ($\text{SiO}_2:\text{C}$) mole ratio. This experiment was to evaluate the possible higher temperature ($\Delta F = 0$ at 3000 K) reaction:



where CO_2 is produced rather than CO.

The product collected from these test runs, although mostly SiO_x , was relatively free of unreacted carbon or silica. Results of tests with variation of feed material composition are reported in section III.G.3.c.

c. Cold Versus Hot Quenching Temperature

A water-cooled copper tube was suspended in the tail flame of the plasma about 7 cm above the work coil. Material which collected as a condensate on the tube varied in color from dark brown near the flame to a light yellow-brown further downstream (up to 30 cm from the work coil) in the quench tube. The material was sintered at 1550°C and analyzed for silicon.

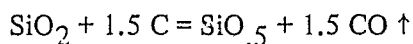
A silicon carbide coated graphite tube was suspended in the tail flame during the reaction and temperatures were measured between 1075°C , at the section where direct impingement of the flame occurred, to 900°C on the tube side opposite to flame impingement. Very little condensate formed on the high-temperature (1075°C) surface of the tube.

An intermediate surface temperature for quenching was investigated by suspending a carbide coated piece of graphite at a distance of approximately 30 cm above the work coil. Temperature was estimated to be between 400°C and 700°C . Material which condensed on this piece of graphite even though it was 30 cm from the work coil was mostly dark brown colored rather than light yellow-brown (which is characteristic of condensate near the exit of the quench tube). An intermediate temperature surface, e.g., above 200°C but below 900°C , may be a preferred quench temperature for the silicon-containing gases.

d. Analysis of Reaction By-Product Gases

Gas chromatography was used to analyze the exhaust gases for the presence of CO or CO_2 . It was verified that the gases generated from the reaction of SiO_2 and carbon contained an amount of CO plus CO_2 (at a specified reactant feed rate) which was equivalent to the stoichiometric volume estimated for a complete conversion of all carbon to CO and CO_2 .

A calculation of the theoretical amount of CO produced based on using batch C-2, which contained 1.5 moles of C (23% by wt) to 1.0 mole of silica, was made assuming the following reaction:



For a reactant feed rate of 0.06 gm per minute, the volume of CO generated would be 25.8 ml per minute in 18 liters of argon. A CO content in the exhaust gases would therefore be 1435 ppm. This agreed very closely with the actual measured quantity of CO and CO₂ in the by-product gases sampled from the reactor quench chamber.

A reaction mechanism in which silicon is produced and vaporized and partially recombines with the excess oxygen and possibly with some of the CO/CO₂ to form a silicon suboxide, is consistent with a low recoverable Si (never greater than 33% by weight) in the sintered condensate.

2. Plan for Experimental Reactor Study

Figure 21 outlines the planned approach to experimental work using the laboratory-scale induction plasma reactor.

3. Matrix of Experiments for Optimization of Variables

a. Design of Statistical Experiments

The experimental design was based on the variation of factors on two levels, for example a maximum and minimum parameter value. In the case where the number of factors is known, it is immediately possible to find the number of trials required for all possible combinations of their levels,²⁰

$$N = 2^k$$

where

N = number of trials

k = number of factors

2 = number of levels

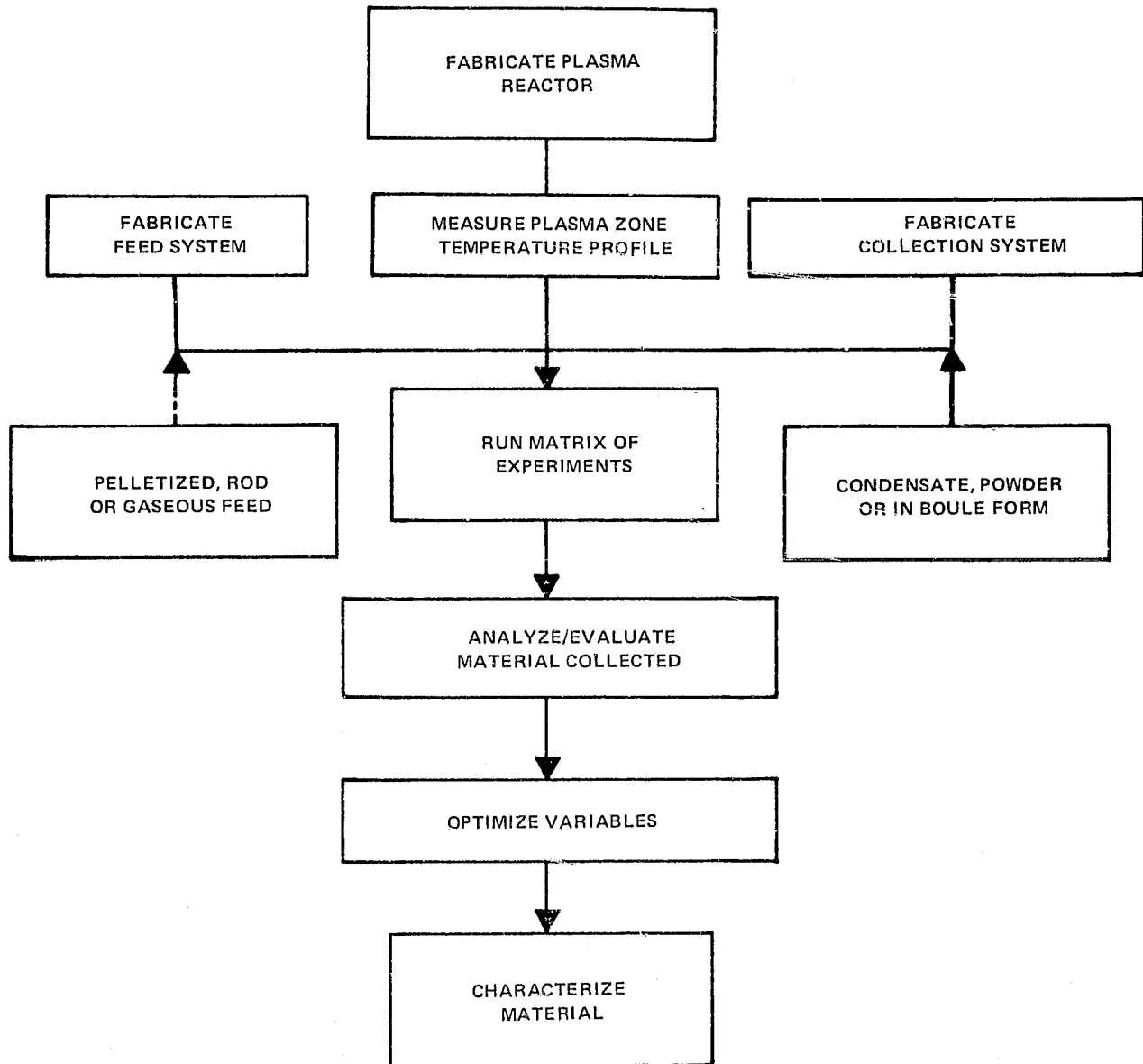


Figure 21. Planned Approach for Reactor Studies

An experiment in which all possible combinations of the factor levels are realized is called a factorial experiment. The factorial experiment $N = 2^3$ which includes eight trials covering all combinations of the two levels (min. and max.) of three factors: power (i.e., temperature), feed rate, and gas flow rate, was chosen. The 2^3 factorial design may be geometrically represented by the coordinates of the vertices of a cube. Using F, G, and P for feed rate of reactants, gas flow rate and power level (temperature) to designate the three major process variables, Figure 22 is a schematic representation of the experiments.

b. Experimental Results

Following the cube diagram (Figure 22), the initial group of 11 runs was made and product was collected, sintered, and analyzed. Composition of feed material was five parts silica to one part carbon, i.e., 1:1 mole ratio, and the extruded rods were 6 mm in diameter. Material condensed on the reactor walls and the quartz tube collector suspended in the quench chamber was weighed and then sintered at 1550°C for one minute to consolidate the powder. Wet chemical analysis gave the percent elemental silicon produced. Results are shown in Table 12.

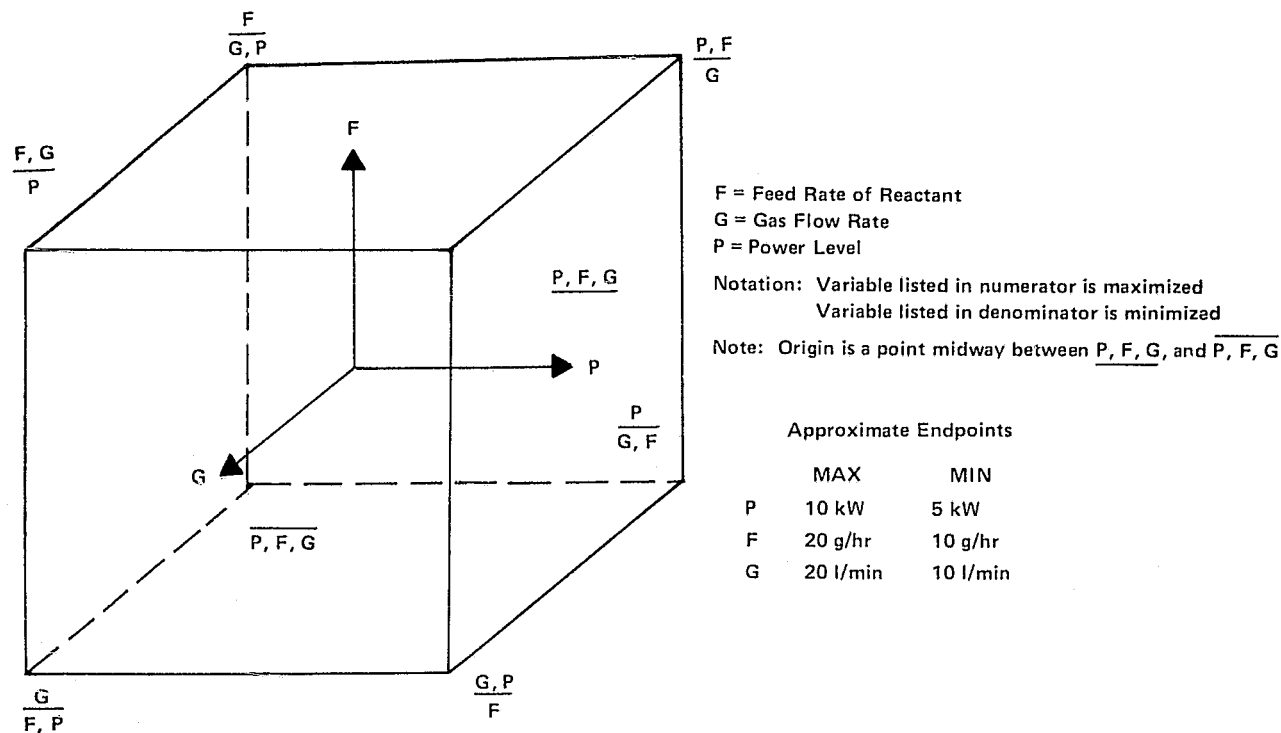


Figure 22. Schematic Representation of Experiments

Table 12. Results of Experiments for Optimization of Variables

Run Designation	Input Power kW	Plasma Gas Flow l/min	Material Feed Rate gm/min	Product Collected %	Silicon In Product %	Comments on Sintered Product and/or Results
$\frac{GP}{F}$	14	3	0.02	25	23	Si globules observed
$\frac{PF}{G}$	14	1	0.05	30	17	Si Globules observed
$\frac{G}{FP}$	7	3	0.02	28	6	SiO ₂ fibers present
$\frac{PFG}{}$	14	3	0.05	68	14	Si globules observed
$\frac{P}{GF}$	14	1	0.02	22	20	Si globules observed
$\frac{FG}{P}$	7	3	0.05	11	—	Plasma flame extinguished
$\frac{GPF}{}$	7	1	0.02	24	3	No Si observed
$\frac{F}{GP}$	7	1	0.05	17	—	Plasma flame extinguished
$\frac{PFG}{2}$	10	2	0.025	<10	—	Insufficient product collected
$\frac{GP}{2} \frac{F}{}$	10	2	0.02	25	9	SiO ₂ fibers present
$\frac{GP}{2} \frac{F}{}$	10	2	0.05	19	10	Si globules observed

- NOTES: 1. Sheath gas was 15 l/min, purge gas was 0.08 l/min.
 2. Run time was 30 minutes.
 3. Feed composition was SiO₂/C (1:1 mole ratio) in rod form.
 4. Sintering was at 1550°C in argon.

The best conditions for process variables for silicon yield were maximum power, maximum plasma gas flow and minimum feed rate. This was run GP/F and silicon was 23% of the sintered product. In fact, the four runs showing the greatest amount of silicon (14% to 23%) were those conducted at maximum power. Where maximum feed rate and minimum power were attempted, the plasma flame could not be sustained, and no silicon was detected in the product from run GPF where all variables were at minimum levels. Intermediate locations were chosen on the cubical matrix, i.e., at the center of the cube body and two face centers. These were midway between minimum-maximum values for all three variables (PFG/2) and for gas flow and material feed rates. Results of these test runs are shown in the last three rows of data in Table 12. The amount of silicon observed in the product was between the minimum and maximum, i.e., approximately 9%, for the runs at the two face center positions.

The total percent of product collected, based upon the amount of material fed to the reactor, was indicative of the efficiency of vaporization of material in the flame. Composition of the product would be more related to the ability of the flame to transfer heat to the feed material, hence to cause the SiO_2 to be reduced to silicon and/or silicon suboxides. The theoretical amount of silicon which could be obtained at 100% reduction of the SiO_2 is $\approx 39\%$ of the starting material mixture. In the case of the GP/F run for example, where 25% product was recovered of which 23% was elemental Si, the yield of silicon would be 15% of theoretical.

A repeat run for conditions corresponding to PFG was made and results of silicon content of product collected was within 20% of the amount found in the original run.

c. Variation of Feed Material Composition

Raw material mixtures of varying carbon-to-silica mole ratios of 1:1 to 2.8:1 were prepared to determine an optimum feed rod composition. The influence of batch preparation procedure and organic binder additions were also investigated. The addition of a binder such as methyl cellulose (Dow Methocel) and polyvinyl alcohol (PVA, Du Pont Grade 70-05) was necessary for extrusion into 6-mm diameter rods. Table 13 lists data and results of experimental runs made with the compositions investigated. Plasma test run conditions were 14 kW input power, 3 liters/min argon plasma gas flow, and varied between minimum feed rate (0.02 gm/min) and maximum feed rate (0.05 gm/min).

Conclusions drawn from these experiments are:

- 1) The carbon content in the reactant feed mixture had the greatest effect of variables investigated. A carbon-to-silica mole ratio between 1.5 and 1.9 to 1.0, i.e., 23% to 27% carbon, appeared to be an optimum composition.
- 2) Wet-milling the raw materials achieved greater particle contact between reactants and more homogeneous batch mixture than does dry milling.
- 3) Source of the silica, Penn. Glass Sand's Supersil or Wedron silica, both in powder form and of equal purity, had little significance on formation of silicon.
- 4) Binder addition was important for plasticity and dry strength of extruded rods, but had little effect on reaction rate or efficiency of silicon formation.

Table 13. Variation in Composition and Batch Preparation of Feed Mixture

Run No.	Batch No.	% Carbon (Including Binder)	C:SiO ₂ Mole Ratio	Batch Preparation Procedure and Binder Addition	% Silicon In Sintered Product	Comments on Product
P-49	B-16	15.6	0.92	Wet-milled. Methocel, PVA.	6	Fused SiO ₂ formed on rod tip. Complete vaporization.
P-52	B-19	21.2	1.34	Wet-milled. Methocel, PVA.	10	SiO ₂ and Si on rod tip. Complete vaporization.
P-44	B-13	22.9	1.48	Wet-milled. PVA.	15	SiO ₂ and Si on rod tip. Complete vaporization.
P-37	C-2	23.4	1.50	Wet-milled. Methocel, PVA. Supersil silica	23	Si formed on rod tip. Complete vaporization.
P-52	B-18	24.5	1.62	Wet-milled. Methocel, PVA.	33	Si formed on rod tip. Complete vaporization.
P-50	B-17	26.8	1.91	Wet-milled. Methocel, PVA.	32	Si formed on rod tip. Incomplete vaporization at accelerated feed rate but conversion to silicon in-situ.
P-41	B-12	28.3	1.97	Wet-milled. PVA.	—	No Si on rod. Insufficient product collected.
P-36	B-10	31.8	2.33	Dry-milled. PVA.	15	Incomplete vaporization. SiC formed on rod.
P-42	B-14	33.2	2.48	Wet-milled. PVA.	—	Incomplete vaporization. SiC formed on rod.
P-39	C-8	35.8	2.78	Wet-milled. Methocel, PVA. Supersil Silica.	—	Rod did not vaporize.

Note: Huber carbon black and Wedron silica were used except where noted.

Binder additions were made to the mill and/or after drying for rod fabrication.

Carbon percentages were determined by ignition test on feed rod.

Run conditions were the same for all experiments except where noted.

d. Product Consolidation and Analysis

The samples of condensed product collected after each test run were heat-treated to consolidate or coalesce the amorphous, low-density, material. The powder was heated in a fused silica liner inside a graphite crucible (≈ 1 inch OD, $1/2$ inch ID) using a resistance heated cold-wall furnace. After closing the furnace and purging with argon, the temperature was raised in 20 minutes to 1550°C and held for one minute before reducing the power. The cool down was to 1000°C in five minutes and then power was cut off for cooling to room temperature.

Wet chemical analysis of the sintered reaction product of earlier (prematrix) scoping experiments showed 28-30% of the total weight of the material collected was silicon. The silicon was visible after consolidation in globular form, Figure 23, with protrusions from the spherical surfaces, characteristic of a material which expands on freezing from the melt. The globules ranged in size from ≈ 25 micrometers to ≈ 250 micrometers.

An emission spectrographic analysis of the silicon indicated at least an order-of-magnitude reduction in content of impurities from the starting materials. Table 14 compares the analysis of the raw material batch with the silicon product.

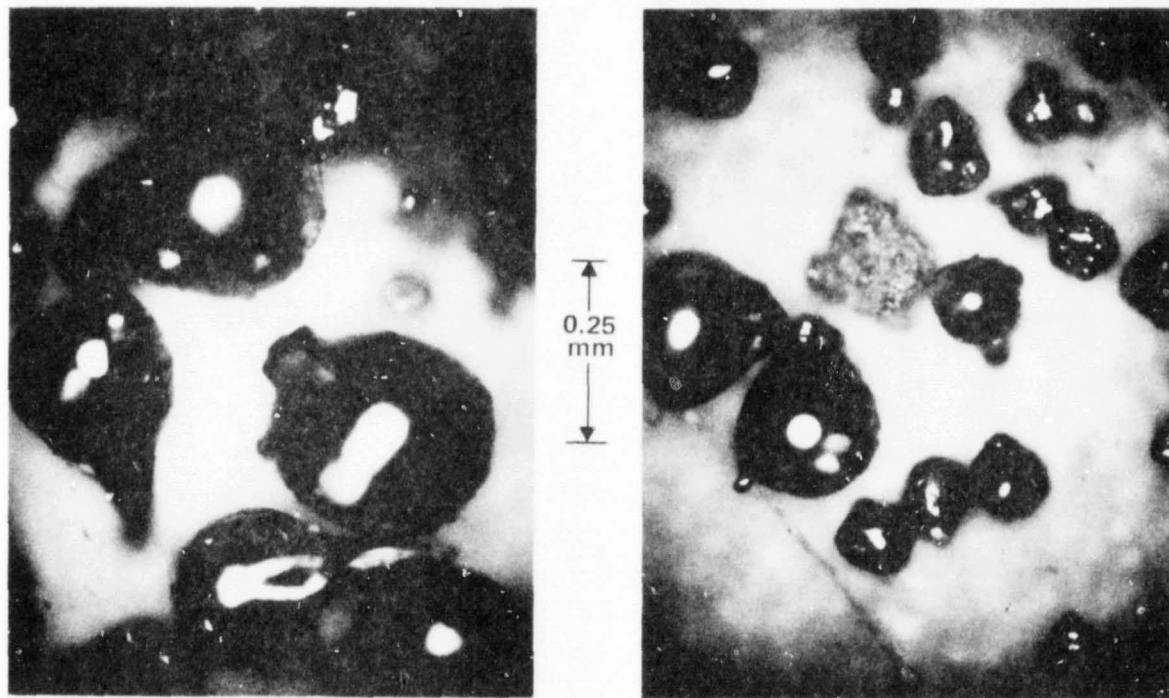


Figure 23. Silicon Globules Produced by Consolidation of Material Collected from Plasma Reaction

Table 14. Emission Spectrographic Analysis of Silicon

	Silicon Product	Raw Batch (SiO ₂ /C)
Fe	10-100 ppm, wt	100-1000 ppm, wt
Mg	3-30	30-300
Al	10-100	300-3000
Ca	10-100	100-1000
Cu	1-10	1-10
Ag	0.1-1	0.1-1
B	ND < 0.15	3-30
P	ND < 1.0	ND < 1.0
Ti	ND < 0.12	30-300
Mn	ND < 0.07	1-10
Ar	ND < 1.0	ND < 1.0
Na	ND < 4.0	100-1000

e. In-Situ Formation of Silicon on Feed Rod

A photograph at 15X magnification of the feed rod tip of Batch B-17, C:SiO₂ ratio 1.9:1 (27% C), from Run No. P-50 is seen in Figure 24. The observation was made that silicon was

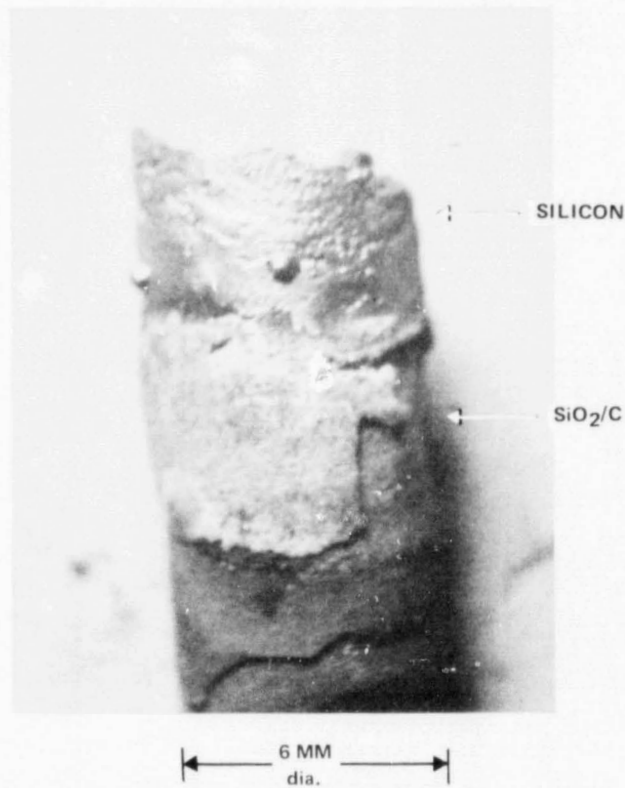


Figure 24. Tip of Feed Rod Converted to Silicon – Run P-50, Batch B-17

forming on the feed rod as it entered the base of the plasma flame on test batches which contained between 1.3:1 to 1.9:1 C to SiO₂ ratio (21% and 27% carbon). The silicon which formed could be seen to boil and vaporize as the rod was progressively fed into the high-temperature core of the flame.

The possibility of collecting material in a liquid form rather than condensing the vaporized silicon by feeding the reactants through the side of the reactor nozzle tube at right angles to the flame was investigated. The liquid silicon formed in the rod of the reactants might coalesce and drip off as the rod penetrated into the flame. This proved unsuccessful. The reaction of the SiO₂/C mixture was minimal in the plasma tail flame, approximately 1/2 cm above the work coil, as the peak temperature at that point was below that required for complete reduction. Another approach might be to use a large inverted reactor and feed the reactants from the top into the flame base. This could allow the silicon which forms to drop off the feed rod before vaporizing and to be collected in some manner below (downstream) as a liquid or solid.

4. Discussion of Results

a. Observations on Quenched Product Characteristics

The material collected in the reactor as condensate from gases produced in the reaction of SiO₂ and carbon in the argon plasma contains much SiO since:

- 1) The color and form are visibly similar to condensed SiO
- 2) HF will dissolve most of the material; therefore, it must contain SiO₂ or SiO
- 3) Amorphous material is detected on the x-ray Debye-Scherrer photograph, and only occasionally is the crystalline form of Si or SiO₂ detected
- 4) Upon heating to the melting point of silicon in an argon atmosphere, the material forms small beads of silicon equivalent to about 30% by weight, thus the SiO may be disproportionating to Si and SiO₂. If silicon alone was present, the bulk of the material would fuse with perhaps a small amount of residue (slag) formation.

Experiments to answer the question of why SiO rather than Si is formed (or collected) on quenching gases from the reaction were performed:

- 1) The nozzle (30-mm diameter) tube was extended and characteristics of material deposited on the tube wall were observed at varying distances from the work coil. With the SiO₂/C mixture (1:1 mole ratio) being vaporized, it was noted that the condensate changed from a dark brown to a lighter yellow-brown color indicating a composition gradation from silicon-rich SiO_x to a material of increasing oxygen content as it deposited further downstream from the high-temperature flame.

- 2) Silica was vaporized with no binder addition in the argon plasma. The material collected nearest the flame was light yellow-brown colored while as the distance from the flame increased the color became white. The observed product color change was caused by SiO_2 dissociating into its atomic species in the high-temperature plasma and material quenched near the flame was SiO_x ($x < 2$), while that which collected downstream at a lower temperature had time to recombine, mostly to SiO_2 .
- 3) The tube wall was externally heated at varying distances from the plasma ball using a H_2 torch and the material which deposited was darker brown colored. The temperature and position above (downstream from) the work coil appeared to be about 10 cm from the coil and a temperature around 600°C for the present apparatus.
- 4) Nitrogen was introduced into the argon plasma to extend the flame length and residence time by dissociation ($\text{N}_2 \rightarrow 2\text{N}$) and ionization ($2\text{N} \rightarrow 2\text{N}^+$) followed by a recombining and evolution of heat. The flame was noticeably lengthened and material collected was gray-white near the coil and gray-brown at some distance (≈ 20 cm) downstream. The presence of Si_3N_4 was detected and would account for the color of the condensed material.

b. Factors Contributing to Silicon Yield

The reaction product from the plasma reactor from SiO_2 -carbon feedstock has consistently been one containing substantial amounts of SiO . This product can be disproportionated to silicon and silicon dioxide.

Several factors were concluded to contribute to collected product being essentially SiO rather than Si . The residence time at the high temperature (> 2500 K) during cool down was insufficient to form a molecular species containing a C-O species, in a redistribution reduction reaction, and silicon vapor. It was observed experimentally that the material collected as condensate from fully vaporized reactants, as in the case where the SiO_2/C mixture is in rod form as it enters the flame, is very similar to that which is formed from particle (pelletized SiO/C mixture) feedstock. Hence, residence time for the reduction reaction to occur between molecular species of Si , O , and C may be less critical than originally assumed.

The situation is made more complex since the reactant concentration in the plasma gas is very low. At the extremely diluted reactant concentration (0.05 gm/min raw material feed rate in 20 liters/minute argon equals 5 carbon, 2.4 silicon and 5 oxygen per 1000 atoms of argon) the collision frequency of reactant species is low in the plasma at the critical cool-down temperature.

Another factor which could contribute to a high concentration of silicon monoxide in the product is the possibility of a reaction occurring between silicon vapor and CO_2 . This reaction is thermodynamically favorable above 1050 K and could contribute to the quantity of SiO collected on quenching. However, CO is the expected species at temperatures where Si is in the vapor state. Controlling the reaction temperature (admittedly difficult to accomplish) and finding the optimum temperature for quenching are required to achieve any significant improvement in silicon yield.

H. H. Kellogg²¹ has remarked that "No reduction process is complete until the metal has been physically separated from the residue." In quenching of the reaction products, the condensation of Si vapor and SiO_2 vapor occur at temperatures of 2953 K and 2503 K respectively, and in attempting to recover Si at a practical quenching temperature, the SiO_2 vapor present will also condense. Thus the separation of Si from SiO_2 which are present in the condensed product, requires further processing. The fact that both condensed materials were present as amorphous, finely divided powder further complicated the separation.

c. Observed Reaction in the Plasma and Interpretation of Reaction Mechanism

Silicon formed on the tip of the rod, provided there was sufficient heat transferable from the flame, and the SiO_2/C mixture was an optimum composition, and includes that particle contact was maximized by fine grinding and efficient homogenization of the raw materials. The type and amount of organic binder added for fabricating the raw materials into an extruded rod may also have had an effect upon the reaction rate.

The silicon formed in the liquid state around 2500 K and was observed to vaporize at or above ≈ 3000 K. If material preparation and/or process parameters (power, reactant feed rate, etc.) are not optimum, the reactants will form SiC and the rod will penetrate the flame without sublimation. The formation of SiC is more likely when concentration of carbon is above 25% by weight in the mixture.

An amorphous material, which is primarily silicon suboxides but may contain some elemental silicon, results upon quenching the vaporized silicon in the presence of CO_2 and CO. The practical problem is rapidly quenching the Si vapor in the immediate vicinity of the high-temperature plasma flame, as the Si is vaporized, before the Si can recombine with the CO_2 or CO. This reverse reaction ($\text{Si} + \text{CO}_2 = \text{SiO} + \text{CO}$) is thermodynamically favorable above 1050 K. The objective then is to reduce the probability of Si recombining with by-product gases by reducing the residence time of the gaseous species (Si, CO, CO_2) at temperatures above 1050 K.

Page intentionally left blank

**SECTION IV
PRELIMINARY ECONOMIC STUDY**

Early in the program, a preliminary estimate of manufacturing costs for a plasma process was made.²² The costs were based on a procedure which assumes that the raw materials could be directly converted at a 35% yield to silicon of sufficient purity to qualify as solar-grade material without further processing. Less than a 35% yield would increase the raw material and other costs proportionately. Capital equipment and production requirements are based on a plant capacity of 3000 metric tons per year, at a production rate of approximately 575 kg per hour. The initial estimate of electrical power required was based on consuming 35 kW hours per kilogram of silicon produced. As the experimental work progressed, and as knowledge about the poor heat transfer efficiency of the plasma was gained, this estimate proved to be about an order of magnitude too low.

Capital Investment	Dollars (000s)
Equipment	10110
Fixed Capital Cost (3 X equip. costs)	30330
Working Capital (0.15 X fixed capital)	<u>4550</u>
Total Capital Costs	34880

Manufacturing Costs

Direct Manufacturing Costs	
Raw Materials	3942
Direct Labor	750
Utilities	3264
R & M	404
Supplies	61
Laboratory	1500
Packing, Shipping	30
Royalties, Patents	600
Supervision	<u>112</u>
Total Direct Manufacturing Costs	10663

Manufacturing Costs (continued)

Dollars (000s)

Indirect Manufacturing Costs	
Plant Payroll Overheat	912
Depreciation, straight line, 10 yrs.	3033
Properties plus Insurance	<u>1213</u>
Total Indirect Manufacturing Costs	5158
Total Manufacturing Costs	15821
Manufacturing Costs, Dollars per kg	5.27
Gross Product Margin (30%)	2.26
Price, Dollars per kg	7.53

SECTION V CRITICAL ASSESSMENT

A. CONTRIBUTIONS

Contributions resulting from the development effort are listed.

- 1) Silicon was produced as a condensate of the silica and carbon reaction as well as "in-situ" in the reactant feed rod.
- 2) The silicon produced was of about two orders of magnitude lower in impurity level than the starting materials (silica and carbon).
- 3) An argon induction plasma did supply a noncontaminating high-temperature heat source for the reduction reaction.
- 4) Contributions to the engineering know-how of plasma reactors as well as a better understanding of the Si-O-C reaction chemistry and plasma reactions generally were made.
- 5) Improved pre-processing techniques of low-impurity raw materials were demonstrated.
- 6) With reasonable projected product yield ($\geq 35\%$ overall), the material economics of the process appear favorable.
- 7) Measurement of CO and CO₂ in exhaust gases by G.C. and analysis of silicon contained in the condensed product support the identified condensed-phase reaction mechanism.

B. IDENTIFIED OBSTACLES

Two major obstacles to achieving a more reasonable degree of success in this program, both of which impact directly on the economics of the process, are the inefficient utilization of energy (kW hr/kg Si produced) and the amount of elemental silicon recoverable in the product. The first problem relates to the poor transfer of heat between the plasma gas and the solid raw materials being reacted. The second problem, namely increasing the silicon yield relates to several fundamental factors, such as residence time, quenching rate, rate of heating, reaction temperature and collection efficiency, each of which required resolution before an economic process could be developed.

Other technical barriers impacting the feasibility of the plasma approach are:

- 1) Energy utilization is extremely inefficient due to poor heat transfer characteristics from gas to solids within the plasma flame.
- 2) The large volume of gases involved make quenching difficult and severely limit the collection of product as a condensate.
- 3) The presence of undesirable by-products and partially reacted raw materials are contaminants which are not economically practical to remove.
- 4) SiO_x formation is excessive and difficult to control.
- 5) Reaction temperatures, e.g., maintaining temperatures between 2500 K and 2900 K, were too difficult to control in the plasma flame.

SECTION VI CONCLUSIONS AND RECOMMENDATIONS

The technical feasibility of producing silicon from the raw materials, silica and carbon black, was demonstrated using a laboratory-scale plasma reactor. Energy utilization was inefficient due to poor heat transfer characteristics of the plasma and yield of silicon in the product collected as condensate was never greater than 33% ($\approx 25\%$ of the stoichiometric amount available). These factors prohibit the economic justification of this approach to a process for producing solar-grade silicon at a low ($< \$10/\text{kg}$) manufacturing cost. The problems related to inefficiency of energy utilization and product yield were not resolvable in this effort.

The condensed-state reaction, i.e., the "in-situ" formation of silicon in the reactant feed rod, would be an alternative approach to investigate. The experimental results suggest that reduction reaction likely occurs while reactants are in a condensed state. Further heating of the rod causes product silicon to vaporize simultaneously with carbon and oxygen containing gases from additional reduction reaction. The high yield recovery by quenching of the product silicon from a highly reactive gas stream, regardless of how the mixture was formed, is unlikely. Alternative approaches which would prevent vaporizing the desired product, such as collecting the silicon liquid formed, have much more potential. For example, an alternative heat source to the use of the induction plasma would be to directly heat the reactant feed rod as illustrated in Figure 25.

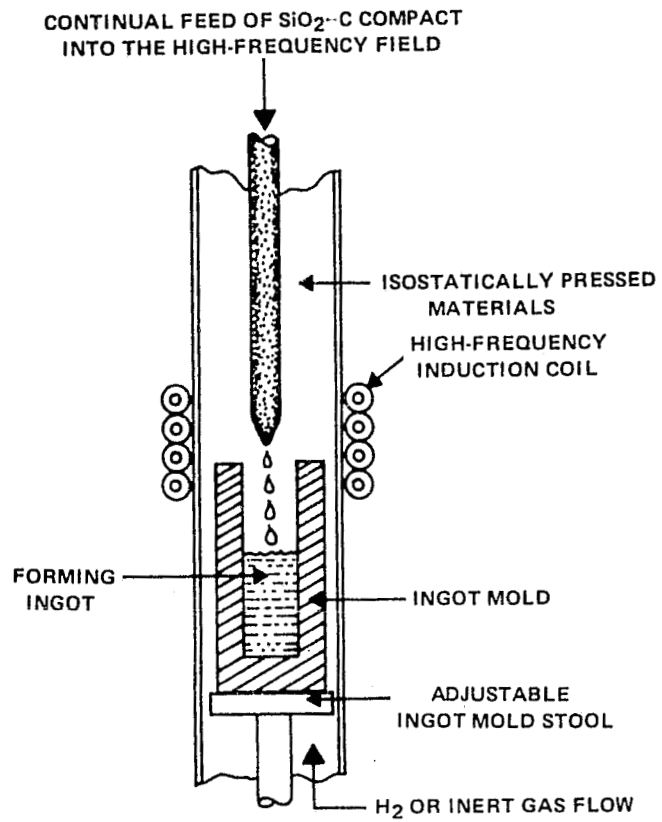


Figure 25. Vertical Induction Furnace for Silicon Smelting Process

SECTION VII
PROGRAM SCHEDULE

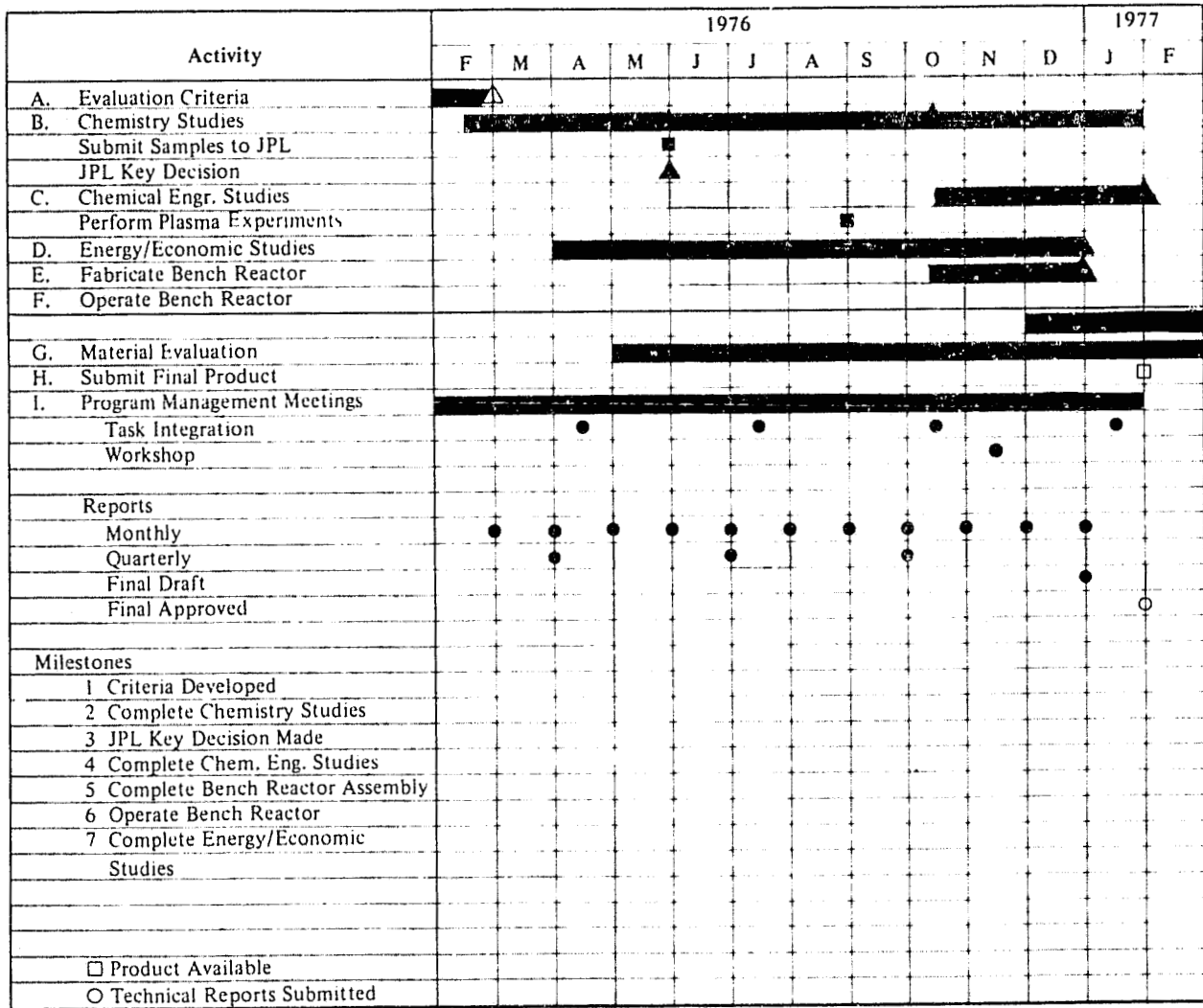


Figure 26. Program Schedule

Page intentionally left blank

SECTION VIII
REFERENCES

1. W. T. Fairchild, *Trans. Met. Soc. AIME*, Paper No. A70-36 (1970).
2. L. P. Hunt, *IEEE Photovoltaic Spec. Conf.* 11, 259 (1975).
3. T. B. Reed, *J. Appl. Phys.* 32, 821 (1961).
4. P. W. J. M. Boumans, F. J. deBoer, and J. W. deRuiter, *Philips Tech. Rev.* 33, 50-59, No. 2 (1973).
5. R. K. Rains and R. H. Kadlec, *Met. Trans.*, Vol. 1, 1501-1506 (1970).
6. K. Nassau and J. W. Shiever, *Bull. Amer. Ceram. Soc.*, Vol. 54, 11, 1004 (1975).
7. R. F. Baddour and R. S. Timmius, *The Application of Plasma to Chemical Processing*, MIT paper (1967).
8. W. T. Fairchild, *Ibid.*
9. D. R. Cruise, *J. Phys. Chem.* 68, 3794 (1964).
10. L. P. Hunt and E. Sirtl, *J. Electrochem. Soc.* 119, 1741 (1972).
11. *JANAF Thermochemical Tables*, Second Edition, NSRDS-NBS37 (1971).
12. T. B. Reed, *Ibid.*
13. D. M. Coldwell, *High Temperature Science* 8, 309 (1976).
14. W. D. Kiistensen, *J. Non-Crystalline Solids* 21, 303 (1976).
15. A. Rahman, *Phys. Rev.* 136, A405 (1964).
16. W. Hertl and W. W. Pultz, *J. Amer. Ceram. Soc.* 50, 378 (1967).

17. R. F. Baddour and R. S. Timmius, *Ibid.*
18. M. P. Freemour and S. Katz, *J. Opt. Soc. Am.* 50, 826 (1960).
19. R. H. Tourin, *Spectroscopic Gas Temperature Measurement* (New York: Elsevier, 1966).
20. Y. P. Adler, E. V. Markova and Y. V. Granovsky, *The Design of Experiments to Find Optimal Condition*, (Moscow: Mir Publishers, 1975).
21. H. H. Kellogg, *Proc. of International Symp. on High Temperature Technology*, 182-191 (New York: McGraw-Hill, 1960).
22. O. Winter, *Ind. and Eng. Chem.*, Vol. 61 (4) (1969).

APPENDIX A EVALUATION CRITERIA

I. RAW MATERIAL SELECTION

A. Sources

Determine cost, availability, and analyses available, especially of boron and phosphorus contents, for silica and carbon black.

B. Theoretical Considerations

Review thermodynamic and kinetic considerations involving effects of raw material composition, temperature, pressure, and residence times including reactions of impurities with carbon at plasma reaction conditions. Assemble the data from the review and use as one of guidelines for selecting raw material candidates.

C. Raw Material Candidates

Select raw material candidates having minimum impurities, especially of boron and phosphorus, that are either removed by the plasma reaction in accordance with theoretical considerations, or are tolerable in the silicon product.

II. RAW MATERIAL PREPARATION

A. Storage and Handling

Establish requirements for ease of handling and prevention of contamination during storage and transportation of both the as-received raw materials and their related pelletized forms.

B. Requirements for Preparation

Establish the requirements for the ranges of sizes, conditions, forms, and proportions of silica-carbon black mixtures and pelletized configurations in accordance with theoretical considerations, laboratory experiments, and the plan for experiments at the vendor's facility.

C. Sizing Experiments

Evaluate the effectiveness of milling on comminution, dispersion, and homogeneity. Visual examination under a microscope (min. 10X) will be used to evaluate the particle size distribution characteristics and chemical analyses will be used for detection of any additional impurities introduced by the sizing process.

D. Condition and Form

Prepare pelletized forms of the silica-carbon black mixture suitable for processing in the TAFA plasma reactor. Qualitatively determine the characteristic features including the surface to volume ratio, size distribution, and strength of the pellets.

III. PLASMA REACTION CHARACTERISTICS

A. Experiments at Vendor's Facility

Describe the experiments and determine the dependence of raw material characteristics, pellet size, durability, etc., on probability of the reaction occurring in the particular plasma reactor under investigation. Optimize whatever parameters are controllable in this cursory study and record their relationship to successfully prove the feasibility of the reaction.

B. Further Process Investigations

1. Experiments With In-House Bench Reactor

Conduct experiments on a laboratory scale with an especially designed and fabricated plasma reactor to provide information regarding the following process variables:

- a. Ratio of $\text{SiO}_2:\text{C}$, i.e., variations from stoichiometry
- b. Feed rate, condition of feed material
- c. Gas flow rate and composition (Ar, N_2 , etc.) for *carrier* gas and *arc* gas(es)
- d. Collection techniques
- e. Temperature/time of reaction, power input, etc.
- f. Exhaust gas environmental impact
- g. Position of feed to plasma flame

- h. Quenching and cooling product and exhaust
- i. Energy usage
- j. Operational safety

2. Product Evaluation

a. *Product Yield*

The end product from the experiments shall be silicon representing at least 50% of that theoretically possible from stoichiometry.

b. *Production Rate*

The goal is to obtain a reaction rate that favorably indicates the feasibility of attaining a production rate of 250 grams of silicon product per hour in a bench scale reactor.

c. *Process Repeatability*

Evaluate the process data for the degree of repeatability when utilizing sets of favorable process parameters.

d. *Product Purity*

The purity of the silicon product shall be equal to or better than that of solar-grade silicon. Until a definition of solar-grade silicon has been established by the LSSA project at JPL, tentative definitions currently in use in the scientific community shall be the criterion.

e. *Composition Analyses*

Product evaluation for chemical composition will be x-ray diffraction for confirming the presence of elemental silicon, by wet chemical analyses for silica determination, and by LECO instrumentation for carbon analysis.

f. *Physical Form*

The silicon product physical form must be found amenable to further processing using existing industry-established techniques.

IV. CONCLUSIONS FROM PRELIMINARY EXPERIMENTS

Derive conclusions from the preliminary experiments that are based on the factors of purity, yield, production rate, cost, energy, environmental impact, and operational safety. The conclusions must be the basis of an acceptable technical argument for proceeding to the bench reactor design and chemical engineering studies.

APPENDIX B
EMISSION SPECTROGRAPHIC DETECTION LIMITS FOR
IMPURITIES IN SILICON AND CARBON
(parts per million weight)

	Si	C
Be	.0005	
B	.15	.08
Na	4.0	.05
Mg	.0003	.006
Al	.2	.06
P	1.0	1.0
Ca		.06
Ti	.12	.08
V	1.1	.06
Cr	2.5	.1
Mn	.07	.02
Fe	.25	.06
Co	.09	.1
Ni	.7	.5
Cu	.07	.03
Zn	1.	1.0
Ga	.05	.05
As	1.	1.0
Sr	.2	.2
Zr	1.5	.5
Mo	.25	.1
Ru	2.	
Rh	.07	.1
Pd	.0095	.09
Ag	.006	.006
In	.015	.02
Sn	1.	.05
Sb	1.	.5
Hf	20.	
Re	2.	
Ir	5	4.0
Pt	.05	.05
Au	.6	.6
Hg	2.	2.0
Pb	.15	.05
Bi	.35	.01
K		.05
Si		.08

APPENDIX C
DETECTION LIMITS FOR IMPURITIES IN SILICON
 (parts per million atomic)

IA		IIA		IIIB		IVB		VB		VIB		VIIB		VIII		IB		IIB		IIIA	IVA	VA	VIA	VIIA	HE
1	H																			B	C	N	O	F	Ne
	Li	Be																		4 x 10 ⁻¹	1 x 10 ⁻¹	2 x 10 ⁻¹	1.0	7 x 10 ⁻³	
2	9 x 10 ⁻²	2 x 10 ⁻³	7 x 10 ⁻³																	8 x 10 ⁻³					
	Na	Mg																		2 x 10 ⁻¹					
3	5	4 x 10 ⁻⁴	7 x 10 ⁻²																	1 x 10 ⁻³					
	7 x 10 ⁻³	4 x 10 ⁻⁴	7 x 10 ⁻²																	2 x 10 ⁻¹					
	2 x 10 ⁻⁴	7 x 10 ⁻²																		1 x 10 ⁻³					
4	K	Ca																		Ca	Ge	As	Se	Br	Kr
	7 x 10 ⁻³	7 x 10 ⁻³	7 x 10 ⁻³	7 x 10 ⁻²	6 x 10 ⁻¹	2	4 x 10 ⁻²	1 x 10 ⁻¹	4 x 10 ⁻²	3 x 10 ⁻¹	3 x 10 ⁻²	4 x 10 ⁻¹	2 x 10 ⁻²	1 x 10 ⁻²	4 x 10 ⁻¹	2 x 10 ⁻²	2 x 10 ⁻²	7 x 10 ⁻³	1 x 10 ⁻²	4 x 10 ⁻⁵	2 x 10 ⁻²	1 x 10 ⁻²	1 x 10 ⁻²		
	1 x 10 ⁻²	5 x 10 ⁻³	2 x 10 ⁻⁵	1 x 10 ⁻¹	7 x 10 ⁻³	8 x 10 ⁻³	7 x 10 ⁻³	1 x 10 ⁻¹	2	2 x 10 ⁻¹	2 x 10 ⁻⁴	3 x 10 ⁻²	2 x 10 ⁻⁴	2 x 10 ⁻⁴	4 x 10 ⁻⁵	2 x 10 ⁻²	2 x 10 ⁻²	1 x 10 ⁻⁵	2 x 10 ⁻³	4 x 10 ⁻⁵	2 x 10 ⁻²	2 x 10 ⁻³	2 x 10 ⁻⁵		
5	Rb	Sr	Y	Zr	Nb	Mo	Tc	Ru	Rh	Pd	Ag	Cd	In	Sn	Sb	Te	I	Xe							
	15	20	50	5 x 10 ⁻¹	7 x 10 ⁻²	3 x 10 ⁻²		6 x 10 ⁻¹	2 x 10 ⁻¹	3 x 10 ⁻¹	2 x 10 ⁻¹	5 x 10 ⁻²	4 x 10 ⁻³	2 x 10 ⁻¹	2 x 10 ⁻¹	1 x 10 ⁻²	2 x 10 ⁻²	7 x 10 ⁻³							
	2 x 10 ⁻³	5 x 10 ⁻²	500	4 x 10 ⁻²	7 x 10 ⁻³	3 x 10 ⁻²		2 x 10 ⁻²	2 x 10 ⁻²	2 x 10 ⁻²	2 x 10 ⁻⁴	2 x 10 ⁻³	2 x 10 ⁻⁴	4 x 10 ⁻⁴	1 x 10 ⁻⁵	2									
6	Ls	Ba	La	Hf	Ta	W	Re	Os	Ir	Pt	Au	Hg	Tl	Pb	Bi	Po	At	Rn							
	7 x 10 ⁻³	1 x 10 ⁻²	7 x 10 ⁻³	3 x 10 ⁻²	1	2 x 10 ⁻²	1 x 10 ⁻²	2 x 10 ⁻²	8 x 10 ⁻¹	7 x 10 ⁻³	7 x 10 ⁻²	3 x 10 ⁻¹		2 x 10 ⁻²	5 x 10 ⁻⁴										
	1 x 10 ⁻⁴	1 x 10 ⁻²	6 x 10 ⁻⁶	3 x 10 ⁻⁵	5 x 10 ⁻⁵	1 x 10 ⁻⁵	3 x 10 ⁻⁶	5 x 10 ⁻⁵	2 x 10 ⁻⁶	2 x 10 ⁻⁶	2 x 10 ⁻⁶	3 x 10 ⁻⁶	1 x 10 ⁻⁶	1 x 10 ⁻²	1 x 10 ⁻²	7 x 10 ⁻³									
7	Fr	Ra	Ac																						

6	Fe	Pb	Hb	Hg	Se	Eu	Co	Ir	By	Hd	Pr	Th	Vh	Lu
	5 x 10 ⁻²	5 x 10 ⁻²	3 x 10 ⁻²		9 x 10 ⁻³	6 x 10 ⁻³	9 x 10 ⁻³	4 x 10 ⁻³	8 x 10 ⁻³	4 x 10 ⁻³	8 x 10 ⁻³	1	3 x 10 ⁻²	5 x 10 ⁻³
	2 x 10 ⁻⁴	2 x 10 ⁻⁴	2 x 10 ⁻⁴		4 x 10 ⁻⁷		2 x 10 ⁻⁴	1 x 10 ⁻⁴	6	2 x 10 ⁻⁶	3 x 10 ⁻⁴	4 x 10 ⁻⁵	1 x 10 ⁻⁵	4 x 10 ⁻⁶
7	Hh	Pa	U											
	6 x 10 ⁻³		6 x 10 ⁻³											

• x 10⁰
 v x 10⁰
 - x 10⁰

EMISSION SPECTROGRAPHIC DETECTION LIMIT
 MASS SPECTROGRAPHIC DETECTION LIMIT
 NEUTRON ACTIVATION ANALYSIS DETECTION LIMIT
 BASED ON 1-GRAM SAMPLE, 14-HR. IRRADIATION
 AT 1.5 x 10¹³ n/sec-cm², 60-HR. DECAY.

C-1

APPENDIX D
PROCEDURE FOR DETERMINATION OF SILICON

Samples were weighed and transferred to 100 ml tripour beakers. Ten milliliters of common oxide etch was added. The solution was then filtered through 8 10 micron Teflon filter to remove SiO₂. The precipitate was dissolved in 10% NaOH and H₂O₂. This solution was heated on the steam bath to remove excess H₂O₂. The solution was then filtered through a 10 micron Teflon filter to remove the SiC and C. The filtrate was diluted to 100 ml. Aliquots of this were used for the analyses.

Standards were prepared containing 30, 45, 60, 75, 112, and 149 μg of Si. One ml of 2% boric acid was added to sample and standards. The pH was adjusted to 1.4 with 9N H₂SO₄. Five milliliters of 10% NH₄ molybdate was added and allowed to stand for 5 minutes. Then 15 ml of 9N H₂SO₄, 10 ml of 4% oxalic acid, and 10 ml or 2.5% Fe (NH₄) SO₄ - 6 H₂O were added. Samples and standards were transferred quantitatively to 100-ml polyethylene volumetric flasks and diluted to volume. Readings were on a Beckman Du-2 at 725 nanometers.

A standard curve was set up plotting micrograms of Si versus absorbance readings. Micrograms of Si in samples were determined from curve.

Calculations

$$\frac{\mu\text{g Si} \times 100 \times 10^{-4}}{\text{ml in aliquot} \times \text{SW}} = \% \text{ Si}$$